Rpgrip1l controls ciliary gating by ensuring the proper amount of Cep290 at the vertebrate transition zone

Antonia Wiegering[a,b], Renate Dildrop[a,†], Christine Vesque[b], Hemant Khanna[c], Sylvie Schneider-Maunoury[b,*], and Christoph Gerhardt[a,*]

[a]Institute for Animal Developmental and Molecular Biology, Heinrich Heine University, 40225 Düsseldorf, Germany; [b]Sorbonne Université, CNRS UMR7622, INSERM U1156, Institut de Biologie Paris Seine (IBPS) – Developmental Biology Unit, 75005 Paris, France; [c]Department of Ophthalmology and Neurobiology, University of Massachusetts Medical School, Worcester, MA 01605

ABSTRACT **A range of severe human diseases called ciliopathies is caused by the dysfunction of primary cilia. Primary cilia are cytoplasmic protrusions consisting of the basal body (BB), the axoneme, and the transition zone (TZ). The BB is a modified mother centriole from which the axoneme, the microtubule-based ciliary scaffold, is formed. At the proximal end of the axoneme, the TZ functions as the ciliary gate governing ciliary protein entry and exit. Since ciliopathies often develop due to mutations in genes encoding proteins that localize to the TZ, the understanding of the mechanisms underlying TZ function is of eminent importance. Here, we show that the ciliopathy protein Rpgrip1l governs ciliary gating by ensuring the proper amount of Cep290 at the vertebrate TZ. Further, we identified the flavonoid eupatilin as a potential agent to tackle ciliopathies caused by mutations in *RPGRIP1L* as it rescues ciliary gating in the absence of Rpgrip1l.**

Monitoring Editor
Francis Barr
University of Oxford

Received: Mar 12, 2020
Revised: Feb 8, 2021
Accepted: Feb 16, 2021

INTRODUCTION

The spatiotemporal regulation of cellular processes such as proliferation, apoptosis, migration, specification, and differentiation depends on the cell's ability to transduce signals from the environment into the cell's interior. In nearly all mammalian cells, the primary cilium is dedicated to signal reception and transduction. Consequently, dysfunctional primary cilia result in severe often deadly human diseases, collectively called ciliopathies (Reiter and Leroux, 2017). The current treatment of ciliopathies is restricted to symptomatic therapies and a curative medication against ciliopathies is missing (McIntyre *et al.*, 2013). In many cases, ciliopathies are caused by mutations in genes encoding transition zone (TZ) proteins (Hildebrandt *et al.*, 2011; Czarnecki and Shah, 2012). As the TZ functions as the ciliary gatekeeper governing ciliary protein import and export (Betleja and Cole, 2010; Craige *et al.*, 2010; Omran, 2010; Benzing and Schermer, 2011; Czarnecki and Shah, 2012; Garcia-Gonzalo and Reiter, 2012; Reiter *et al.*, 2012; Garcia-Gonzalo and Reiter, 2017; Jensen and Leroux, 2017), a defective TZ can affect the proper formation of cilia and alter the transduction of signaling pathways (Reiter and Skarnes, 2006; Vierkotten *et al.*, 2007; Chih *et al.*, 2011; Garcia-Gonzalo *et al.*, 2011; Williams *et al.*, 2011; Warburton-Pitt *et al.*, 2012; Jensen *et al.*, 2015; Yee *et al.*, 2015; Li *et al.*, 2016; Shi *et al.*, 2017; Weng *et al.*, 2018; Lewis *et al.*, 2019). Thus, the investigation of the molecular mechanisms underlying TZ function is an important prerequisite for the development of curative ciliopathy therapies.

In this study, we shed light on the role of Rpgrip1l in regulating the ciliary gating function of the TZ. Our previous investigations revealed that mutations in *RPGRIP1L* cause deadly ciliopathies (Delous *et al.*, 2007), that Rpgrip1l localizes to the vertebrate TZ (Gerhardt *et al.*, 2015), and that it is a decisive factor in vertebrate TZ

This article was published online ahead of print in MBoC in Press (http://www.molbiolcell.org/cgi/doi/10.1091/mbc.E20-03-0190) on February 24, 2021.

†Present address: Institute of Genetics, Heinrich Heine University, 40225 Düsseldorf, Germany.

*Address correspondence to: Christoph Gerhardt (Christoph.Gerhardt@hhu.de); Sylvie Schneider-Maunoury (sylvie.schneider-maunoury@upmc.fr).

Abbreviations used: Ac3, adenylate cyclase 3; ANOVA, analysis of variance; Arl13b, ADP ribosylation factor-like GTPase 13B; BB, basal body; BBS, Bardet-Biedl syndrome; Cspp1, centrosome and spindle pole-associated protein 1; Cep, centrosomal protein; FCS, fetal calf serum; HSD, honest significance difference; Invs, Inversin; MEF, mouse embryonic fibroblast; Nphp, nephrocystin; PBS, phosphate-buffered saline; PCM1, pericentriolar material 1; RPE, retinal pigment epithelial; Sept, septin; Smo, smoothened; Sstr3, somatostatin receptor 3; SSX2IP, SSX family member 2 interacting protein; TF-Ctrl, transfection control; TZ, transition zone.

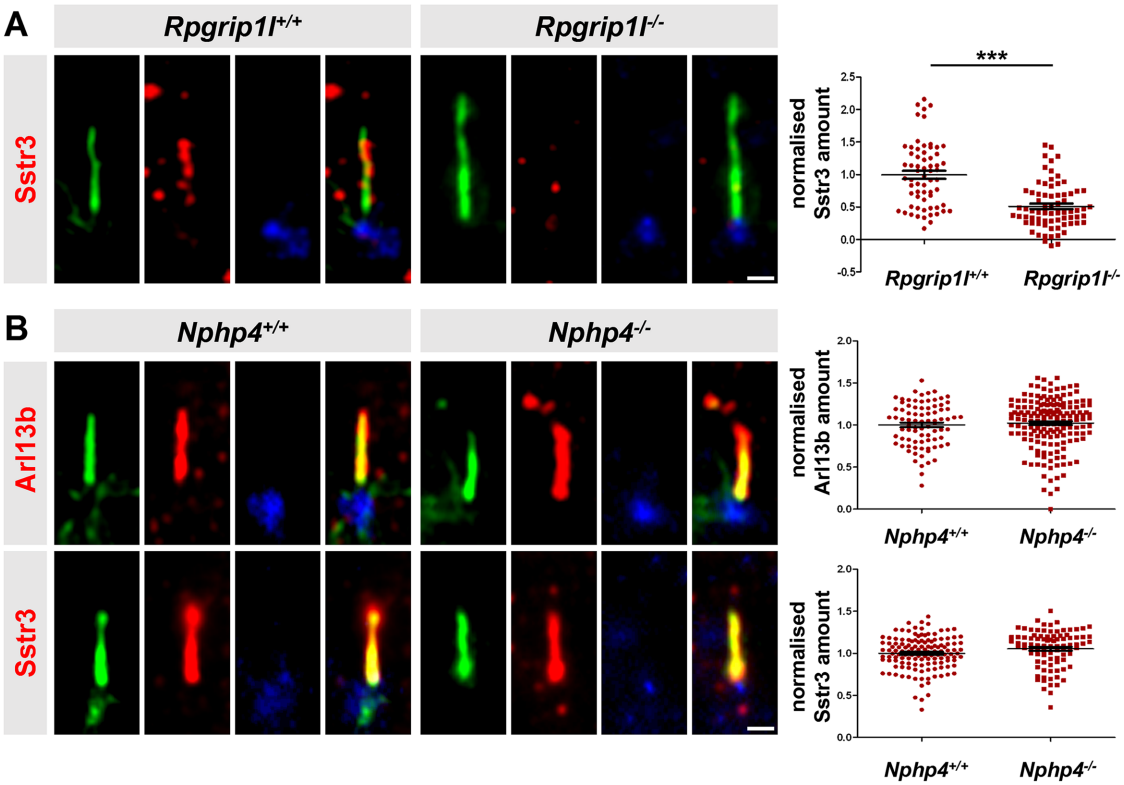

FIGURE 1: In mouse cells, ciliary gating is disturbed by the loss of Rpgrip1l but not by the loss of Nphp4. (A) Immunofluorescence on MEFs obtained from WT ($n = 5$) and *Rpgrip1l*$^{-/-}$ ($n = 5$) embryos. At least 10 cilia per embryo were used for quantifications (Σ(WT) = 62 cilia, Σ(*Rpgrip1l*$^{-/-}$) = 72 cilia). (B) Immunofluorescence on MEFs obtained from WT (Arl13b: $n = 4$; Sstr3: $n = 3$) and *Nphp4*$^{-/-}$ (Arl13b: $n = 4$; Sstr3: $n = 3$) embryos. At least 20 cilia per embryo were used for quantifications (Arl13b: Σ(WT) = 83 cilia, Σ(*Nphp4*$^{-/-}$) = 171 cilia; Sstr3: Σ(WT) = 134 cilia, Σ(*Nphp4*$^{-/-}$) = 92 cilia). (A, B) The ciliary axoneme is stained in green by acetylated α-tubulin, the BB is stained in blue by γ-tubulin. The scale bars represent a length of 0.5 µm. Data are shown as mean ± SEM. Asterisks denote statistical significance according unpaired *t* tests with Welch´s correction (***$P < 0.001$) (A: t (25) = 6.54, $P < 0.0001$; B: Arl13b: t (46) = 0.7483, $P < 0.4581$; Sstr3: t (80) = 1.807, $P < 0.0745$).

assembly (Wiegering *et al.*, 2018a). Our current work demonstrates that Rpgrip1l deficiency results in an altered ciliary protein composition and that Rpgrip1l governs ciliary gating by ensuring the proper amount of Cep290 at the vertebrate TZ. Further, we revealed that the flavonoid eupatilin rescues ciliary gating in the absence of Rpgrip1l. Consequently, eupatilin might represent a potential agent for the development of therapies against ciliopathies caused by mutations in *RPGRIP1L*.

RESULTS

Rpgrip1l and Cep290 but not nephrocystin (Nphp)1, Nphp4, and Inversin (Invs) function as ciliary gatekeepers in mouse embryonic fibroblasts (MEFs)

Among the proteins allowed to cross the TZ are receptors and mediators of signaling pathways essential for proper development. Examples for such proteins are ADP ribosylation factor-like GTPase 13B (Arl13b), somatostatin receptor 3 (Sstr3), smoothened (Smo), polycystin 2, or adenylate cyclase 3 (Ac3) which are often used as indicators to evaluate whether the gate function of the TZ is impaired (Hu *et al.*, 2010; Chih *et al.*, 2011; Garcia-Gonzalo *et al.*, 2011; Roberson *et al.*, 2015; Li *et al.*, 2016; Shi *et al.*, 2017; Takao *et al.*, 2017; Ye *et al.*, 2018). In a former study, we showed that Rpgrip1l deficiency leads to a reduction of the ciliary Arl13b amount in all analyzed mouse cells in vitro and in vivo (in MEFs, in mouse embryonic kidneys, and in mouse limb buds; Wiegering *et al.*, 2018a). However, we could not detect an alteration of the ciliary Smo amount in *Rpgrip1l*$^{-/-}$ MEFs (Gerhardt *et al.*, 2015), raising the question whether the effect of Rpgrip1l is Arl13b-specific or whether it functions as a more general ciliary gatekeeper at the vertebrate TZ. To answer this question, we analyzed the ciliary Sstr3 amount. It has been known for a long time that Sstr3 localizes to cilia of neuronal cells (Händel *et al.*, 1999). More recently, it was shown that Sstr3 is also present in cilia of retinal pigment epithelial (RPE-1) cells (Klinger *et al.*, 2014). We were now able to visualize endogenous Sstr3 in cilia of MEFs. Importantly, the amount of Sstr3 was decreased in *Rpgrip1l*$^{-/-}$ MEFs (Figure 1A) demonstrating that Rpgrip1l exerts a TZ gatekeeper function.

We next aimed to investigate how Rpgrip1l implements this function. Several proteins function as ciliary gatekeepers and it is an important task to unveil possible relationships between these gatekeeper proteins in order to understand the mechanisms that govern ciliary protein composition. In this context, centrosome and spindle pole-associated protein 1 (Cspp1) was an interesting object of investigation because its truncation in humans results in a reduced ciliary amount of Arl13b and Ac3 (Tuz *et al.*, 2014) and because it interacts with Rpgrip1l (Patzke *et al.*, 2010; Gerhardt *et al.*, 2015). Previously, we and others reported that Rpgrip1l ensures the proper amount of many proteins at the base of vertebrate cilia (Shi *et al.*, 2017; Wiegering *et al.*, 2018a), suggesting that it serves as a vital scaffold protein. Thus, we quantified the

amount of Cspp1 at the ciliary base of *Rpgrip1l*$^{-/-}$ MEFs but we could not detect any alteration (Supplemental Figure S1A), indicating that Rpgrip1l exerts its ciliary gatekeeper function independently of Cspp1. Recently, a potential link between Rpgrip1l and the septin proteins was discussed (Patnaik *et al.*, 2018). Septins are known ciliary gatekeepers in vertebrates localizing at the proximal end of the axoneme in MEFs (Hu *et al.*, 2010). We measured the ciliary amount of two different septins, Septin 2 (Sept2) and Septin 7 (Sept7), in *Rpgrip1l*$^{-/-}$ MEFs. Neither Sept2 nor Sept7 was altered by the loss of Rpgrip1l (Supplemental Figure S1, B and C). We then turned to the TZ proteins Nphp4, Nphp1, centrosomal protein 290 (Cep290) and Invs whose amount at the vertebrate TZ is decreased in the absence of Rpgrip1l (Wiegering *et al.*, 2018a). Previous studies in the invertebrates *Chlamydomonas reinhardtii* and/or *Caenorhabditis elegans* demonstrated that ciliary gating is regulated by the TZ proteins Nphp4, Nphp1, Cep290, and Invs (Craige *et al.*, 2010; Williams *et al.*, 2011; Warburton-Pitt *et al.*, 2012; Awata *et al.*, 2014; Li *et al.*, 2016), raising the possibility that Rpgrip1l might govern ciliary gating by controlling the amount of one of these proteins at the TZ. However, it is unknown whether these proteins function as ciliary gatekeepers in vertebrates and hence we quantified the ciliary amount of Arl13b and Sstr3 in *Nphp4*$^{-/-}$, *Nphp1*$^{-/-}$, *Cep290*$^{-/-}$, and *Invs*$^{-/-}$ mouse cells. The ciliary amount of both Arl13b and Sstr3 was unaffected in *Nphp4*$^{-/-}$ MEFs (Figure 1B). To analyze TZ assembly, we had previously inactivated *Nphp1*, *Cep290*, and *Invs* in NIH3T3 cells (immortalized MEFs; Wiegering *et al.*, 2018a). In the current study, we used these cells to investigate a possible involvement of these proteins in ciliary gating. To be able to perform comparative analyses in this context, we also inactivated Rpgrip1l in NIH3T3 cells (Supplemental Figure S2). As observed in MEFs (Gerhardt *et al.*, 2015), ciliary length was increased in *Rpgrip1l*$^{-/-}$ NIH3T3 cells (Supplemental Figure S2C). Moreover, the ciliary amount of Arl13b and Sstr3 was decreased in *Rpgrip1l*$^{-/-}$ NIH3T3 cells (Figure 2, A and B). In contrast to these cells, *Nphp1*$^{-/-}$ and *Invs*$^{-/-}$ NIH3T3 cells did not show an altered ciliary amount of Arl13b and Sstr3 (Figure 2, A and B) indicating that the decreased amount of Nphp1 and Invs in *Rpgrip1l*$^{-/-}$ MEFs is not the reason for the reduced ciliary Arl13b and Sstr3 amount. Importantly, Cep290 deficiency causes a decrease of the ciliary Arl13b and Sstr3 amount (Figure 2, A and B) making it conceivable that the reduced amount of Cep290 might provoke the diminished amount of Arl13b and Sstr3 in the absence of Rpgrip1l.

Restoration of the Cep290 amount at the TZ of *Rpgrip1l*$^{-/-}$ NIH3T3 and *RPGRIP1L*$^{-/-}$ HEK293 cells rescues the ciliary Arl13b and Sstr3 amount

To test this hypothesis, we enhanced the amount of Cep290 at the TZ of *Rpgrip1l*$^{-/-}$ NIH3T3 cells by transfecting a plasmid that encodes a Flag-mCep290 fusion protein. In addition, to test for the conservation of the functional relationship between these two TZ proteins in humans, we transfected a plasmid that encodes a GFP-hCEP290 fusion protein into *RPGRIP1L*$^{-/-}$ HEK293 cells. In a previous study, we revealed a reduced amount of Cep290 at the TZ of *Rpgrip1l*$^{-/-}$ MEFs and *RPGRIP1L*$^{-/-}$ HEK293 cells (Wiegering *et al.*, 2018a). In line with this, a reduction of Cep290 at the ciliary TZ of *Rpgrip1l*$^{-/-}$ NIH3T3 cells was observed in the present study (Supplemental Figure S4, E and F). In NIH3T3 and HEK293 cells, the transfected Cep290 fusion protein was located at the TZ (Supplemental Figure S4, A and H). In contrast to the Flag-mCep290 fusion protein in NIH3T3 cells and the GFP-hCEP290 fusion protein in HEK293 cells, we could not detect a transfected Myc-mNphp1 fusion protein at the TZ of *Rpgrip1l*$^{-/-}$ NIH3T3 or *RPGRIP1L*$^{-/-}$ HEK293 cells (Supplemental Figure S3). Most likely, Rpgrip1l functions as a TZ scaffold for Nphp1 but not for Cep290.

The transfection of the plasmid encoding the Flag-mCep290 fusion protein into *Rpgrip1l*$^{-/-}$ NIH3T3 cells as well as the transfection of the plasmid encoding the GFP-hCEP290 fusion protein into *RPGRIP1L*$^{-/-}$ HEK293 cells at least partially restored the amount of Cep290 at the TZ (Supplemental Figure S4, E, F, K, and L). Importantly, the rescued amount of Cep290 restored the ciliary amount of Arl13b and Sstr3 in *Rpgrip1l*$^{-/-}$ NIH3T3 (Figure 3, A–C) and the ciliary amount of Arl13b in *RPGRIP1L*$^{-/-}$ HEK293 cells (Figure 3, D and E). HEK293 cells lack Sstr3, preventing the analysis of its localization in the absence of RPGRIP1L and its rescue by CEP290 overexpression (War and Kumar, 2012). Our results indicate that Rpgrip1l controls ciliary gating via ensuring the proper amount of Cep290 at the TZ, both in mouse and human cells.

Cilia of NIH3T3 and HEK293 cells are elongated by the loss of Rpgrip1l (Wiegering *et al.*, 2018a) (Supplemental Figure S4, C and J). Interestingly, the increased cilia length in the absence of Rpgrip1l was not rescued by the expression of the Flag-mCep290 fusion protein in *Rpgrip1l*$^{-/-}$ NIH3T3 cells or the GFP-hCEP290 fusion protein in *RPGRIP1L*$^{-/-}$ HEK293 cells (Supplemental Figure S4, C and J). Thus, contrary to its ciliary gating function, the role of Rpgrip1l in controlling ciliary length is not mediated by Cep290.

To verify the functionality of the Cep290 fusion protein, we transfected the plasmid encoding Flag-mCep290 into *Cep290*$^{-/-}$ NIH3T3 cells. The transfected Cep290 fusion protein was located at the TZ in *Cep290*$^{-/-}$ NIH3T3 cells (Supplemental Figure S4A) and the amount of Cep290 at the TZ was restored (Supplemental Figure S4, E and G). Moreover, the decreased cilia length observed in the absence of Cep290 (Wiegering *et al.*, 2018a) was rescued by the expression of the Flag-mCep290 fusion protein (Supplemental Figure S4D), demonstrating the functionality of the transfected protein in NIH3T3 cells.

Eupatilin treatment rescues ciliary gating in Rpgrip1l-negative MEFs

A recent report showed that eupatilin rescues ciliary gating in *CEP290*$^{-/-}$ human cells by replacing the function of CEP290 in TZ recruitment of Nphp 5 (NPHP5; alias IQCB1) (Kim *et al.*, 2018). Since we showed above that Rpgrip1l function on ciliary gating was mediated by the control of Cep290 TZ amounts, we hypothesized that eupatilin would also rescue the ciliary gating defect in Rpgrip1l-deficient cells. Indeed, the treatment of *Rpgrip1l*$^{-/-}$ NIH3T3 cells with eupatilin restored the ciliary amount of both Arl13b and Sstr3 (Figure 4, A, B, and D), confirming our hypothesis. The enhanced cilia length in *Rpgrip1l*$^{-/-}$ NIH3T3 cells was not rescued by eupatilin (Figure 4I). We also verified that eupatilin treatment of *Cep290*$^{-/-}$ NIH3T3 cells restored the reduced amount of Arl13b and Sstr3 (Figure 4, A, C, and E), but not ciliary length alteration (Figure 4J), in these cells. Furthermore, we analyzed the TZ amount of Nphp5 and found that it was significantly reduced in both *Rpgrip1l*$^{-/-}$ and *Cep290*$^{-/-}$ NIH3T3 cells (Figure 4, F–H). Eupatilin treatment rescued the amount of Nphp5 completely in *Rpgrip1l*$^{-/-}$ NIH3T3 cells (Figure 4G) and more partially in *Cep290*$^{-/-}$ NIH3T3 cells (Figure 4H). Thus, we conclude that Rpgrip1l functions in ciliary gating upstream of Nphp5, via ensuring the proper amount of Cep290 at the TZ.

DISCUSSION

Primary cilia mediate numerous signaling pathways thereby ensuring proper development and homeostasis. In this context, the intraciliary concentration of proteins involved in these signaling pathways is of enormous importance. Consequently, ciliary import

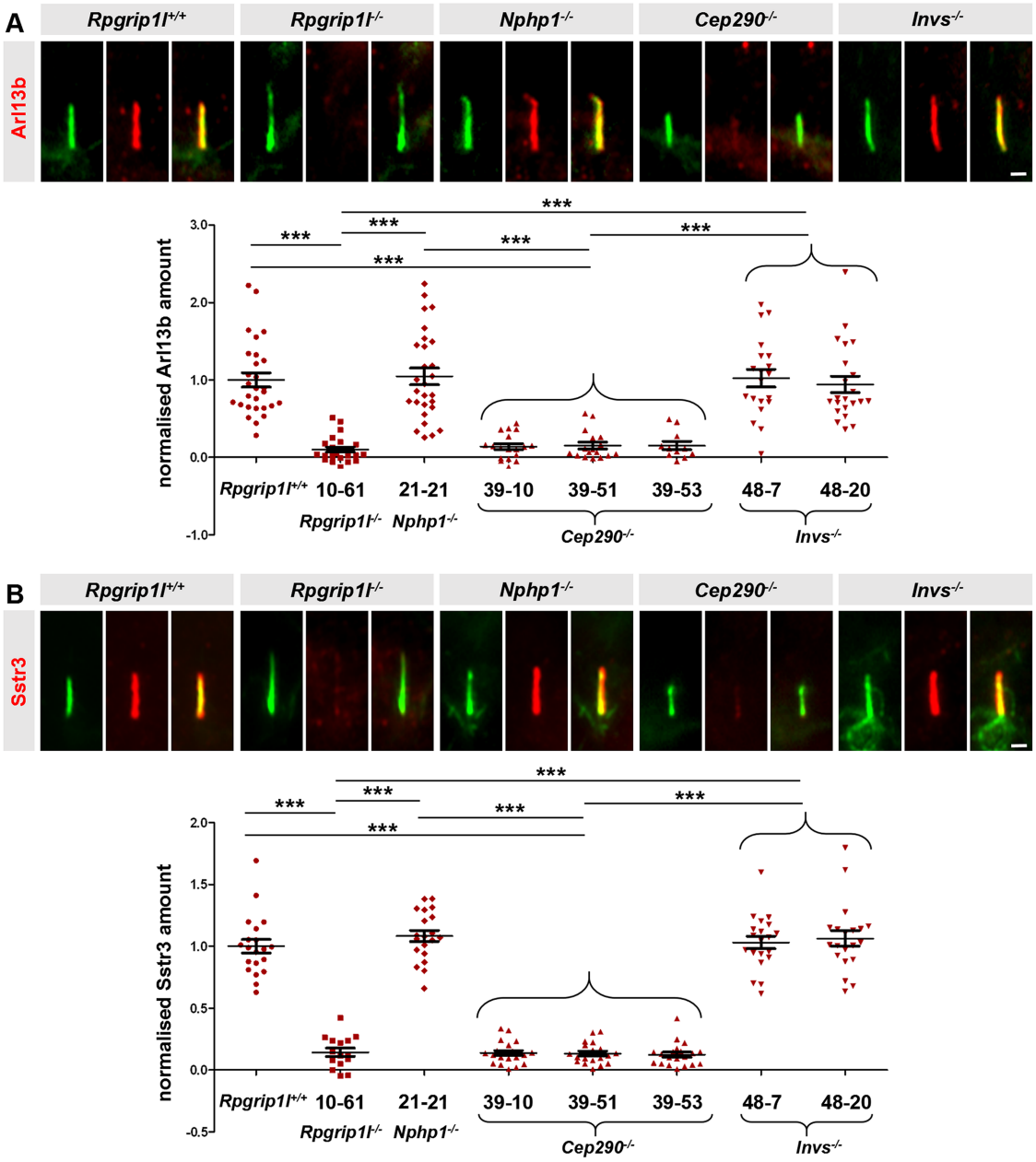

FIGURE 2: Loss of Cep290 but not of Nphp1 or Invs impairs ciliary gating in mouse cells. (A, B) Immunofluorescence on NIH3T3 cells. The ciliary axoneme is stained in green by acetylated α-tubulin. The scale bars represent a length of 0.5 µm. At least 20 cilia per clone were used for quantification. Data are shown as mean ± SEM. Asterisks denote statistical significance according to one-way ANOVA and Tukey HSD tests (***$P < 0.001$) (A: $F(7,160) = 26.09$, $P < 0.0001$; B: $F(7,147) = 133.6$, $P < 0.0001$).

and export and hence ciliary protein composition has to be tightly controlled. This control is implemented by the TZ. Since mutations in genes encoding TZ proteins result in ciliopathies (Hildebrandt *et al.*, 2011; Czarnecki and Shah, 2012; Reiter and Leroux, 2017), current cilia research aims to uncover mechanisms underlying TZ assembly and function. However, little is known about these mechanisms in vertebrates. Recently, we described Rpgrip1l as a decisive factor in vertebrate TZ assembly (Wiegering *et al.*, 2018a). In this context, Rpgrip1l deficiency leads to a reduced amount of Cep290, Nphp1, Nphp4, and Invs at the TZ (Wiegering *et al.*, 2018a). Rpgrip1l, Cep290, Nphp1, Nphp4, and Invs were previously shown to govern ciliary gating in *C. reinhardtii* and/or *C. elegans* (Craige *et al.*, 2010; Williams *et al.*, 2011; Warburton-Pitt *et al.*, 2012; Awata *et al.*, 2014; Li *et al.*, 2016; Lin *et al.*, 2018). However, loss of Nphp1, Nphp4, and Invs did not alter the ciliary amount of Arl13b or Sstr3 in MEFs and NIH3T3 cells (Figures 1B and 2), indicating that they are not involved in gating these proteins in vertebrate primary cilia. Remarkably, several reports point to cell type-specific functions of some TZ proteins (Garcia-Gonzalo *et al.*, 2011; Rachel *et al.*, 2015; Lambacher *et al.*, 2016; Wiegering *et al.*, 2018a; Lewis *et al.*, 2019) making a potential regulation of ciliary gating by Nphp1, Nphp4, and Invs in other vertebrate cell types conceivable. *Rpgrip1l*$^{-/-}$ and *Cep290*$^{-/-}$ mice have a much more severe phenotype than *Nphp1*$^{-/-}$, *Nphp4*$^{-/-}$ and *Invs*$^{-/-}$ mice

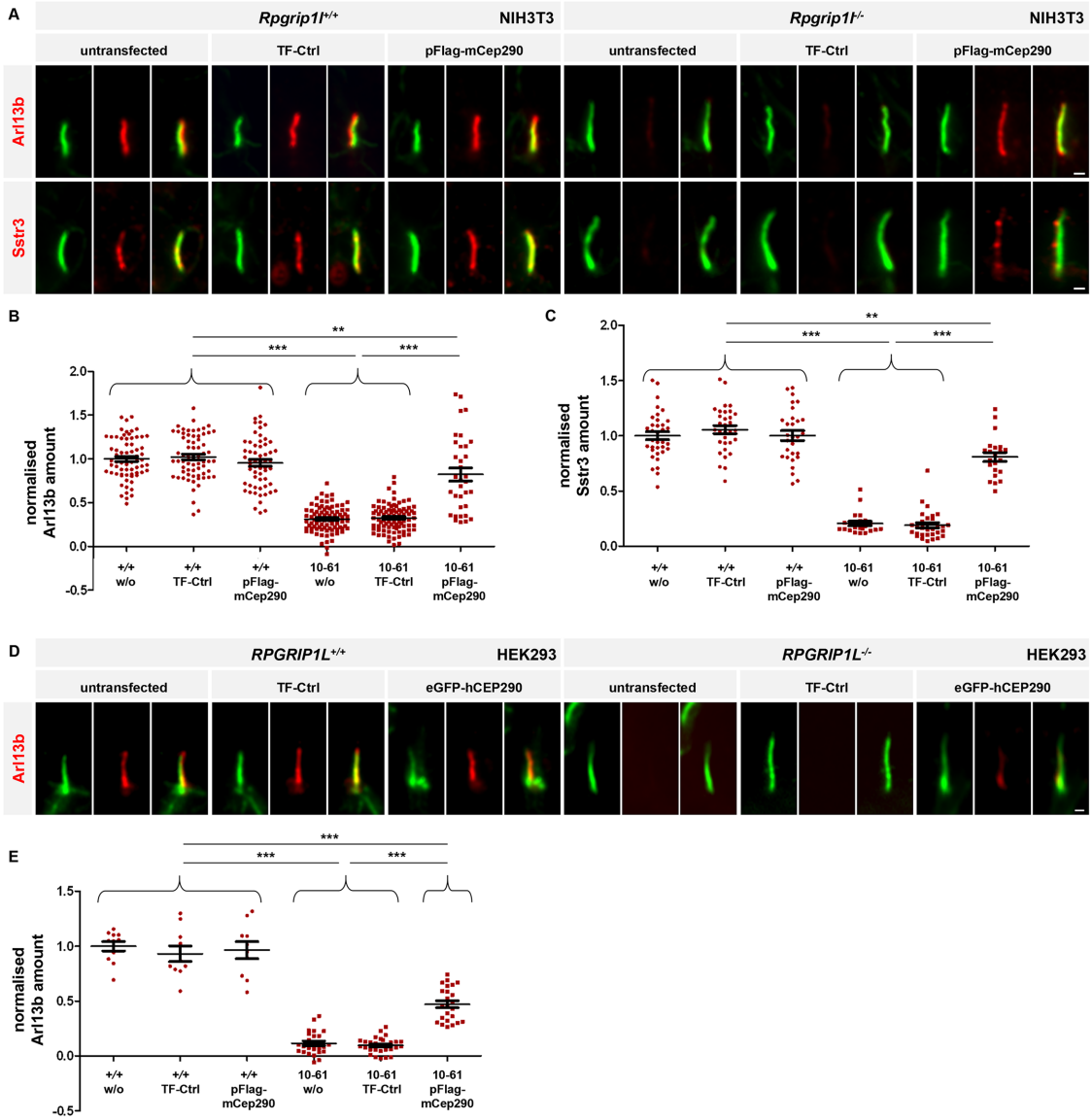

FIGURE 3: Rescue of the Cep290 amount at the TZ of *Rpgrip1l*$^{-/-}$ NIH3T3 and *RPGRIP1L*$^{-/-}$ HEK293 cells restores the ciliary Arl13b and Sstr3 amount. (A–C) *Rpgrip1l*$^{+/+}$ and *Rpgrip1l*$^{-/-}$ NIH3T3 cells were either untransfected or transfected with TF-Ctrl or pFlag-mCep290. (A) Immunofluorescence on *Rpgrip1l*$^{+/+}$ and *Rpgrip1l*$^{-/-}$ (clone 10-61) NIH3T3 cells. The ciliary axoneme is stained in green by acetylated α-tubulin and Arl13b or Sstr3 is stained in red. The scale bars represent a length of 0.5 µm. (B, C) Normalized ciliary amount of Arl13b (B) and Sstr3 (C). At least 30 cilia per clone were used for quantification. Data are shown as mean ± SEM. Asterisks denote statistical significance according to one-way ANOVA and Tukey HSD tests (**$P < 0.01$; ***$P < 0.001$) (B: F (5, 400) = 146.8, $P < 0.0001$; C: F (5, 166) = 128.6, $P < 0.0001$). (D, E) *RPGRIP1L*$^{+/+}$ and *RPGRIP1L*$^{-/-}$ HEK293 cells were either untransfected or transfected with eGFP-hCEP290 or TF-Ctrl. (D) Immunofluorescence on *RPGRIP1L*$^{+/+}$ and *RPGRIP1L*$^{-/-}$ (clone 1–7) HEK293 cells. The ciliary axoneme is stained in green by acetylated α-tubulin and Arl13b is stained in red. The scale bars represent a length of 0.5 µm. (E) Normalized ciliary amount of Arl13b. At least 10 cilia (*RPGRIP1L*$^{+/+}$HEK293 cells) or 20 cilia (*RPGRIP1L*$^{-/-}$ HEK293 cells) per clone were used for quantification. Data are shown as mean ± SEM. Asterisks denote statistical significance according to one-way ANOVA and Tukey HSD tests (***$P < 0.001$) (F (5, 104) = 142, $P < 0.0001$).

(Mochizuki *et al.*, 1998; Morgan *et al.*, 1998; Chang *et al.*, 2006; Delous *et al.*, 2007; McEwen *et al.*, 2007; Vierkotten *et al.*, 2007; Jiang *et al.*, 2008; Jiang *et al.*, 2009; Louie *et al.*, 2010; Besse *et al.*, 2011; Lancaster *et al.*, 2011; Won *et al.*, 2011; Gerhardt *et al.*, 2013; Hynes *et al.*, 2014; Chen *et al.*, 2015; Laclef *et al.*, 2015; Li *et al.*, 2015; Rachel *et al.*, 2015; Wiegering *et al.*, 2018a; Andreu-Cervera *et al.*, 2019; Choi *et al.*, 2019). Moreover, mutations in *RPGRIP1L* and *CEP290* result in more severe human ciliopathies than mutations in *NPHP1*, *NPHP4*, or *INVS* (Zaghloul and Katsanis, 2010; Szymanska and Johnson, 2012; Madhivanan and Aguilar, 2014; Mitchison and Valente, 2017). On the one hand, these differences might reflect that Rpgrip1l and Cep290 function as ciliary gatekeepers in vertebrates while Nphp1, Nphp4, and Invs do not. On the other hand, these differences might be based on the fact that Rpgrip1l and Cep290 exert additional functions in the cytoplasm, for example, the regulation of protein degradation systems (Gerhardt *et al.*, 2015; Struchtrup *et al.*, 2018) or the organization of the cytoplasmic microtubule network (Kim *et al.*, 2008).

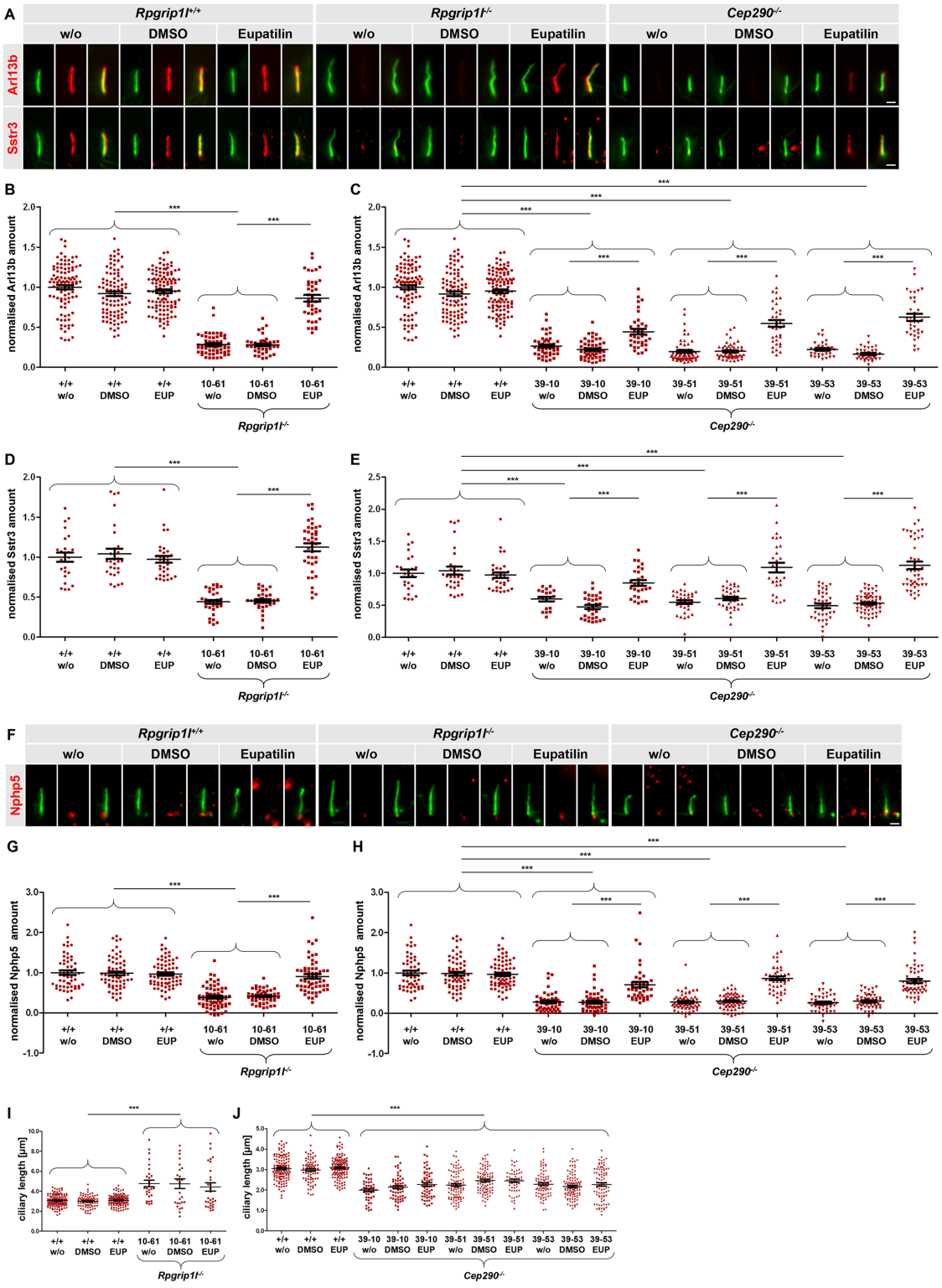

FIGURE 4: Eupatilin treatment rescues ciliary gating in the absence of Rpgrip1l. (A, B) Immunofluorescence on *Rpgrip1l*$^{+/+}$, *Rpgrip1l*$^{-/-}$ (clone 10-61) and *Cep290*$^{-/-}$ NIH3T3 cells. The ciliary axoneme is stained in green by acetylated α-tubulin. Arl13b or Sstr3 is stained in red. The scale bars represent a length of 1 µm. (B–E) Normalized ciliary amount of Arl13b (B, C) and Sstr3 (D, E). At least 20 (D, E) or 30 cilia (B, C) per clone were used for quantification. The same quantification of WT serves as comparison to Rpgri1l-negative and Cep290-negative cells, respectively (B and C; D and E). Data are shown as mean ± SEM. Asterisks denote statistical significance according to one-way ANOVA and Tukey HSD tests (***$P < 0.001$) (B: $F(5, 447) = 117.1$, $P < 0.0001$; C: $F(11, 690) = 163.4$, $P < 0.0001$; D: $F(5, 183) = 47.48$, $P < 0.0001$; E: $F(11, 393) = 35.27$, $P < 0.0001$). (F) Immunofluorescence on *Rpgrip1l*$^{+/+}$, *Rpgrip1l*$^{-/-}$ (clone 10-61) and *Cep290*$^{-/-}$ (clones 39-10, 39-51, 39-53) NIH3T3 cells. The ciliary axoneme is stained in green by acetylated α-tubulin. Nphp5 is stained in red. The scale bars represent a length of 1 µm. (G, H) Normalized ciliary amount of Nphp5. At least

Rpgrip1l does not function as scaffold for Cep290 and Cspp1 at the TZ

Formerly, we demonstrated that Rpgrip1l deficiency does not affect the overall cellular amount of Cep290 but its proper amount at the vertebrate TZ (Wiegering *et al.*, 2018a). There is a perennial debate about the function(s) of Rpgrip1l. Does it predominantly serve as a structural TZ anchor or scaffold protein and interacts with other proteins, thereby ensuring their localization and proper amount at the TZ, or does it control the TZ localization and amount of proteins by exerting additional functions, for example, regulating protein degradation systems, functioning as a TZ assembly factor, establishing a ciliary zone of exclusion that excludes signal transduction proteins, etc. (Coene *et al.*, 2011; Williams *et al.*, 2011; Gerhardt *et al.*, 2015; Jensen *et al.*, 2015; Assis *et al.*, 2017; Shi *et al.*, 2017; Struchtrup *et al.*, 2018; Wiegering *et al.*, 2018a; Wiegering *et al.*, 2018b)? In this study, the Flag-mCep290 and the GFP-hCEP290 fusion proteins were able to localize to the TZ in the absence of Rpgrip1l (Supplemental Figure S4, A and H), indicating that Rpgrip1l does not function as a structural scaffold for the TZ presence of Cep290. In line with this assumption, it was not shown yet that Rpgrip1l interacts with Cep290. To stress this point, we also transfected a plasmid encoding a Myc-mNphp1 fusion protein into *Rpgrip1l*$^{-/-}$ NIH3T3 and *RPGRIP1L*$^{-/-}$ HEK293 cells (Supplemental Figure S3). It was reported before that Nphp1 interacts with Rpgrip1l (Sang *et al.*, 2011). Since Myc-mNphp1 was not present at the TZ in the absence of Rpgrip1l (Supplemental Figure S3, B and D), we suggest that Rpgrip1l functions as a structural anchor for Nphp1 but not for Cep290. The mechanism by which Rpgrip1l regulates the TZ amount of Cep290 is thus not understood, and it will be an exciting future challenge to address this question.

For example, it would be conceivable that Rpgrip1l regulates the amount of Cep290 via interaction with centriolar satellites. It is predicted that Cep290 is part of a satellite subnetwork consisting of pericentriolar material 1 (PCM1), SSX family member 2 interacting protein (SSX2IP), orofaciaodigital syndrome protein 1 (OFD1, centriole and centriolar satellite protein), synaptic vesicle glycoprotein 2B (SV2B; also known as KIAA0735), and CEP290 (Gupta *et al.*, 2015), and that Rpgrip1l is a potential interaction partner of this satellite subnetwork by interacting at least with PCM1 and SSX2IP (Gupta *et al.*, 2015). PCM1 is a major component of centriolar satellites involved in the recruitment of Ceps such as centrin and ninein as well as the organization of a cytoplasmic microtubule network (Kubo *et al.*, 1999; Dammermann and Merdes, 2002; Kubo and Tsukita, 2003). Several studies have shown physical and functional interactions between PCM1 and CEP290 (Chang *et al.*, 2006; Kim *et al.*, 2008; Gupta *et al.*, 2015). However, the loss of PCM1 decreases the localization of CEP290 at centriolar satellites but does not affect the centrosomal/basal body (BB) accumulation of CEP290 (Kim *et al.*, 2008; Stowe *et al.*, 2012; Odabasi *et al.*, 2019). In contrast to that, loss of SSX2IP leads to a reduced amount of CEP290 at the TZ (Klinger *et al.*, 2014). SSX2IP is known to be involved in microtubule anchoring, centrosome maturation, and ciliogenesis as well as being an important effector protein in the FOXJ1 regulatory network (Bärenz *et al.*, 2013; Hori *et al.*, 2014; Hori *et al.*, 2015; Mukherjee *et al.*, 2019). On ciliogenesis, SSX2IP accumulates around the BB (Klinger *et al.*, 2014) and loss of SSX2IP decreases ciliary length in RPE-1 cells (Hori *et al.*, 2014; Klinger *et al.*, 2014). Taken together, Rpgrip1l could regulate the TZ amount of Cep290 by directly regulating SSX2IP, which in turn regulates Cep290.

It was shown before that the proper amount of Rpgrip1l at the TZ depends on Cspp1 and that Rpgrip1l and Cspp1 are directly interacting (Patzke *et al.*, 2010). Moreover, mutations in *CSPP1* disturb ciliary protein composition (e.g., reduced ciliary Arl13b amount; Tuz *et al.*, 2014) and cause Joubert syndrome and Meckel syndrome (Shaheen *et al.*, 2014). Interestingly, Rpgrip1l was not required for the ciliary localization of Cspp1 (Supplemental Figure S1A). Based on these facts, we propose that Cspp1 is at the top of the "ciliary gating hierarchy," and it would be an interesting future task to monitor if gating defects in Cspp1-negative cells are indeed mediated by a decreased TZ amount of Rpgrip1l.

Rpgrip1l controls ciliary gating via Cep290

Here we show that Rpgrip1l controls ciliary gating via ensuring the proper amount of Cep290 at the TZ (Figure 3). The role of Cep290 in ciliary gating is addressed by several studies in which a reduced amount of ciliary membrane proteins like Arl13b and Ac3 in the absence of Cep290 has been shown (Craige *et al.*, 2010; Li *et al.*, 2016; Shimada *et al.*, 2017; Kilander *et al.*, 2018; Kim *et al.*, 2018; Molinari *et al.*, 2019). How Cep290 implements this function is not yet clearly understood, but it was shown that Cep290 governs ciliary protein composition by interacting with Nphp5 (Barbelanne *et al.*, 2015a; Li *et al.*, 2016; Shimada *et al.*, 2017; Kim *et al.*, 2018). Cep290 binds Nphp5 thereby covering the calmodulin binding of Nphp5 and promoting the recruitment of Nphp5 to the TZ (Kim *et al.*, 2018). In the absence of Cep290, the Nphp5 amount at the TZ is reduced, and this amount is restored by eupatilin treatment, which inhibits calmodulin binding to Nphp5 (Kim *et al.*, 2018). In our study, we observed a similar rescue of ciliary amounts of Arl13b and Sstr3, and of Nphp5 TZ amounts, by eupatilin treatment in Rpgrip1l-deficient cells (Figure 4). Together with the rescue of the Arl13b and Sstr3 amount by transfection of tagged Cep290 (Figure 3), these data underpin our assertion that Rpgrip1l exerts is gatekeeper function via Cep290 and Nphp5 (Figure 5). Interestingly, the phenotype of Nphp5-negative mice is not as striking as the phenotype of Cep290-mutant or Rpgrip1l-mutant mice, raising the question whether ciliary gating can really be regulated by Nphp5. Nonetheless, it was shown that the phenotype of Nphp5-mutant mice shows similarities to the phenotype of Cep290-mutant mice and that patients with mutations in *NPHP5* can develop similar ciliopathy syndromes than patients with mutations in *CEP290* (Otto *et al.*, 2005; Chang *et al.*, 2006; Helou *et al.*, 2007; Stone *et al.*, 2011; Ronquillo *et al.*, 2016). It was also shown that the interaction of Cep290 and Nphp5 is required for ciliogenesis (Barbelanne *et al.*, 2013) and that Nphp5 as well as Cep290 regulates components of the BBSome (octameric protein complex consisting of Bardet-Biedl syndrome) (Barbelanne *et al.*, 2015a). In addition, Nphp5 interacts with components of the exocyst complex, a protein complex involved in exocytosis and thereby ciliogenesis (Zuo *et al.*, 2009;

40 cilia per clone were used for quantification. The same quantification of WT serves as comparison to Rpgrip1l-negative and Cep290-negative cells. Data are shown as mean ± SEM. Asterisks denote statistical significance according to one-way ANOVA and Tukey HSD tests (***$P < 0.001$) (G: F (5, 354) = 44.34, $P < 0.0001$; H: F (11, 638) = 64.13, $P < 0.0001$). (I, J) Ciliary length measurements. At least 30 cilia (I) or 50 cilia (J) per clone were used for quantification. The same quantification of the WT serves as comparison to Rpgrip1l-negative and Cep290-negative cells. Data are shown as mean ± SEM. Asterisks denote statistical significance according to one-way ANOVA and Tukey HSD tests (***$P < 0.001$) (I: F (5, 402) = 28.71, $P < 0.0001$; J: F (11, 986) = 36,73, $P < 0.0001$).

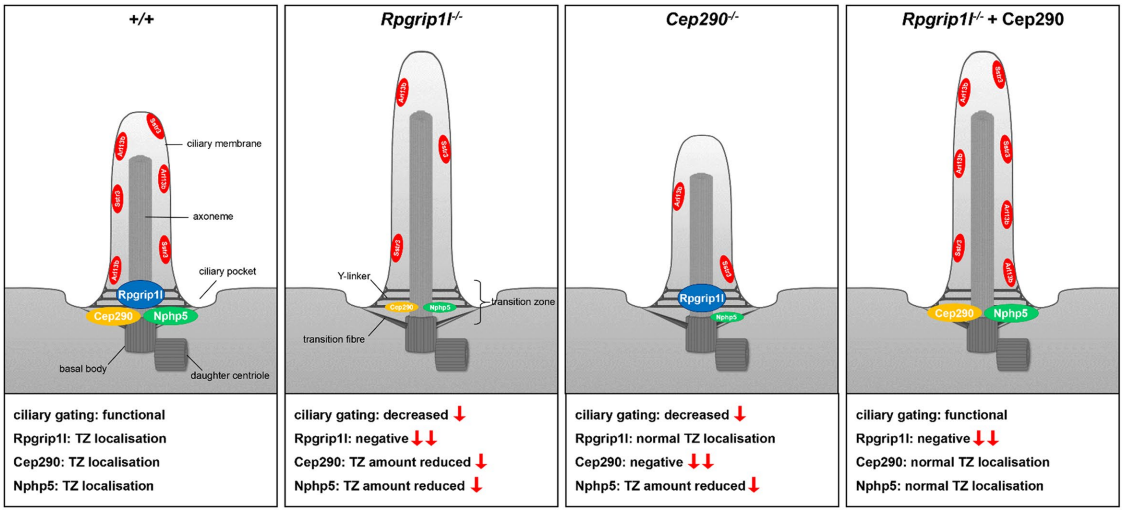

FIGURE 5: Graphical abstract of ciliary gating defects and their rescue in Rpgrip1l- and Cep290-negative NIH3T3 cells. Rpgrip1l controls ciliary gating via ensuring the proper amount of Cep290 at the TZ, which in turn regulates the ciliary amount of Nphp5. In the absence of Rpgrip1l, the ciliary amount of Cep290 and Nphp5 is reduced. This leads to ciliary gating defects indicated by lower ciliary Arl13b and Sstr3 levels. In Cep290-negative cells, the ciliary amount of Rpgrip1l is unaltered, whereas the ciliary amount of Nphp5 is reduced. This leads to down-regulation of ciliary gating in *Cep290*$^{-/-}$ cells. Restoration of the Cep290 amount in *Rpgrip1l*$^{-/-}$ cells via transfection of full-length Cep290 rescues ciliary gating defects. We propose that the rescue of ciliary gating in transfected *Rpgrip1l*$^{-/-}$cells is mediated by a restored ciliary amount of Nphp5.

Sang *et al.*, 2011). Together with the fact we have previously discussed in this paper, that Cep290 and Rpgrip1l exert additional function that may lead to more severe phenotypes in these mutants, it is conceivable that the gating defect in *Rpgrip1l*- and *Cep290*-negative cells is actually mediated by Nphp5.

Taken together, our results show that eupatilin may serve as a potential agent for the treatment of ciliopathies caused by mutations in *RPGRIP1L* and *CEP290*. We assume that the rescue of the ciliary gating defect in patients with variants of *RPGRIP1L* and *CEP290* would bring enormous benefits, even though it may only represent one part of the complex disease pattern. To further validate this treatment strategy, we propose to test the eupatilin treatment in in vivo models by treating *Rpgrip1l*$^{-/-}$ and *Cep290*$^{-/-}$ mouse embryos in utero or ex vivo.

Ciliary length control and ciliary gating is mediated by different mechanisms

Strikingly, the ciliary length alterations in Rpgrip1l-deficient cells were not rescued by the eupatilin treatment (Figure 4I) or by the transfection of Cep290 fusion proteins (Supplemental Figure S4, C and J), indicating that ciliary length alterations and ciliary gating defects are caused by different mechanisms. Ciliogenesis and the associated regulation of ciliary length involve complex regulatory mechanisms that have been intensively studied but are not yet well understood. Many studies have investigated mechanisms involved in timing of cilium formation, cilium maintenance, and cilium disassembly, highlighting the importance of the control of the cell cycle and the conversion of centrioles into BBs, vesicle and membrane trafficking, IFT machinery, ciliary gating, as well as actin-based regulation mechanisms (Ishikawa and Marshall, 2011; Avasthi and Marshall, 2012; Keeling *et al.*, 2016; Wang and Dynlacht, 2018; Copeland, 2020; Kumar and Reiter, 2020).

Taking into consideration that *Rpgrip1l*-mutant and *Cep290*-mutant NIH3T3 cells feature opposite ciliary length alterations (Figures 4, I and J and Supplemental Figure S4, C and D), which probably cannot be explained by the corresponding defect in ciliary gating, different mechanisms have to be affected in the respective mutant. It has been shown that Cep290 regulates ciliary localization of BBS4 via interaction with PCM-1, thereby regulating BBSome integrity and ciliary trafficking (Stowe *et al.*, 2012; Klinger *et al.*, 2014; Kobayashi *et al.*, 2014; Barbelanne *et al.*, 2015a). In this context, Cep290 is involved in the recruitment of the small GTPase Rab8 to the cilium. Rab8 regulates vesicle trafficking and has been shown to collaborate with the BBS protein complex involved in ciliary membrane formation (Nachury *et al.*, 2007; Yoshimura *et al.*, 2007; Kim *et al.*, 2008; Tsang *et al.*, 2008). Taken together, the reduction of ciliary length in *Cep290*$^{-/-}$ NIH3T3 cells could result from a failed recruitment of BBSome components and Rab8 followed by a misregulated vesicle trafficking and disrupted ciliary membrane elongation. In this regard, the reduction of Cep290 at the TZ in *Rpgrip1l*$^{-/-}$ NIH3T3 cells by around 50% does not seem strong enough to disrupt Cep290-dependent vesicle trafficking and ciliary membrane elongation in this mutant.

Instead it has been shown that Rpgrip1l interacts with Myosin Va (Assis *et al.*, 2017), a motor protein required for preciliary vesicle transportation to the mother centriole during ciliogenesis (Wu *et al.*, 2018). The loss of Myosin Va leads to decreased ciliogenesis in RPE-1 and murine inner medullary collecting duct (IMCD3) cells and it is assumed that an increased Myosin Va amount at the ciliary base leads to elongated cilia (Assis *et al.*, 2017; Kohli *et al.*, 2017; Copeland, 2020). As we discussed in a previous study (Wiegering *et al.*, 2018b), mammalian Myosin Va is closely related to Myosin V in *Drosophila melanogaster* (Bonafé and Sellers, 1998). Myosin V is a substrate of proteasomal degradation (Pocha *et al.*, 2011), making it very likely that Myosin Va is likewise degraded by the proteasome. Since Rpgrip1l regulates the proteasome specifically at the ciliary base (Gerhardt *et al.*, 2015), Rpgrip1l could regulate the degradation of Myosin Va via the ciliary proteasome. A loss of Rpgrip1l would lead to an increased amount of Myosin Va at the ciliary base, resulting in an increased vesicle transport during ciliogenesis and an

increased ciliary length. Remarkably, we previously showed that Rpgrip1l deficiency leads to a reduced autophagic activity and that the treatment of Rpgrip1l$^{-/-}$ MEFs with autophagy activators rescues cilia length (Struchtrup *et al.*, 2018). For this reason, Rpgrip1l might regulate cilia length by controlling autophagy. Investigating the complex mechanisms of ciliogenesis will be a major task for the future of cilia research.

The role of TZ proteins in ciliary gating

Interestingly, Garcia-Gonzalo *et al.* revealed that the loss of the TZ gatekeeper protein Tmem67 diminishes the ciliary amount of Arl13b and Ac3 but the ciliary amount of Smo remains normal (Garcia-Gonzalo *et al.*, 2011), demonstrating the existence of a specificity between the gatekeeper proteins and the proteins which are allowed to cross the TZ. In *Rpgrip1l*$^{-/-}$ MEFs, the ciliary amount of Smo is also unaltered (Gerhardt *et al.*, 2015). The lack of Cep290 and Nphp5 in RPE-1 cells results in a reduced ciliary amount of Smo (Barbelanne *et al.*, 2015b). Since the amount of Cep290 is reduced in *Rpgrip1l*$^{-/-}$ MEFs (Wiegering *et al.*, 2018a), the expectation would be that the amount of Smo was decreased in these MEFs. However, these findings have been made in different cell types making it possible that the ciliary gating function of these proteins might be cell type specific. The analysis of this hypothesis is an exciting subject of future studies which would shed further light on the ciliary gating function of the TZ.

Many ciliopathies can be attributed to mutations in genes encoding TZ proteins (Hildebrandt *et al.*, 2011; Czarnecki and Shah, 2012). For this reason, the assembly and function of the TZ is a hot topic in biomedical research. A lot of proteins participate in TZ assembly and/or function as ciliary gatekeepers at the TZ (Craige *et al.*, 2010; Chih *et al.*, 2011; Garcia-Gonzalo *et al.*, 2011; Huang *et al.*, 2011; Sang *et al.*, 2011; Williams *et al.*, 2011; Aubusson-Fleury *et al.*, 2012; Cevik *et al.*, 2013; Wang *et al.*, 2013; Awata *et al.*, 2014; Basiri *et al.*, 2014; Klinger *et al.*, 2014; Tuz *et al.*, 2014; Bachmann-Gagescu *et al.*, 2015; Barbelanne *et al.*, 2015b; Damerla *et al.*, 2015; Roberson *et al.*, 2015; Yee *et al.*, 2015; Lambacher *et al.*, 2016; Li *et al.*, 2016; Pratt *et al.*, 2016; Slaats *et al.*, 2016; Vieillard *et al.*, 2016; Wei *et al.*, 2016; Dyson *et al.*, 2017; Lu *et al.*, 2017; Schou *et al.*, 2017; Shi *et al.*, 2017; Takao *et al.*, 2017; Jensen *et al.*, 2018; Scheidel and Blacque, 2018; Wiegering *et al.*, 2018a; Jack *et al.*, 2019; Lapart *et al.*, 2019; Lewis *et al.*, 2019). However, the relationships between these proteins and hence the mechanisms underlying ciliary gating at the TZ remain largely elusive. Recently, we showed that Rpgrip1l represents a central factor in vertebrate TZ assembly (Wiegering *et al.*, 2018a). Our current study reveals that Rpgrip1l also regulates ciliary gating by ensuring the proper amount of Cep290 at the vertebrate TZ. Combining our results with previous findings, we suggest a protein hierarchy regulating ciliary gating in which Cspp1, Rpgrip1l, Cep290, and Nphp5 are involved. Our work is an important piece of a puzzle depicting this fundamental ciliary process. The completion of this puzzle will be one of the most important tasks of cilia research in the next few years.

MATERIALS AND METHODS

Request a protocol through *Bio-protocol*.

See Table 1 for key resources.

Cell lines

We used two different cell lines in this study. NIH3T3 cells (#ACC59) and HEK293 cells (#ACC35) were both purchased by the German Collection of Microorganisms and Cell Cultures GmbH (DSMZ). Cells were grown in DMEM supplemented with 10% fetal calf serum (FCS), 1/100 (vol/vol) L-glutamine (Life Technologies), 1/100 (vol/vol) sodium pyruvate (Life Technologies), 1/100 (vol/vol) nonessential amino acids (Life Technologies), and 1/100 (vol/vol) pen/strep (Life Technologies) at 37°C and 5% CO_2. The following clones were used: *Rpgrip1l*$^{-/-}$ NIH3T3 cells (clone 10-61), *Cep290*$^{-/-}$ NIH3T3 cells (clones 39-10, 39-51, 39-53) (Wiegering *et al.*, 2018a), *Nphp1*$^{-/-}$ NIH3T3 cells (clone 21-21) (Wiegering *et al.*, 2018a), *Invs*$^{-/-}$ NIH3T3 cells (clones 48-7, 48-20) (Wiegering *et al.*, 2018a), and *RPGRIP1L*$^{-/-}$ HEK293 cells (clone 1-7) (Wiegering *et al.*, 2018a).

Primary cell culture

We isolated MEFs from single mouse embryos (male and female) at embryonic stage (E) 12.5 after standard procedures. MEFs were grown in DMEM supplemented with 10% FCS, 1/100 (vol/vol) L-glutamine (Life Technologies), 1/100 (vol/vol) sodium pyruvate (Life Technologies), 1/100 (vol/vol) nonessential amino acids (Life Technologies), and 1/100 (vol/vol) pen/strep (Life Technologies) at 37°C and 5% CO_2. The following mutant mice were used: *Rpgrip1l*-mutant mice on a C3H-background (Vierkotten *et al.*, 2007) and *Nphp4*-mutant mice on a C57BL/6J-background (Wiegering *et al.*, 2018a).

Cell culture, transfection, and drug treatment

Ciliogenesis in confluent-grown MEFs and NIH3T3 cells was induced by serum starvation (0.5% FCS) for at least 24 h. For DNA transfection, Lipofectamin 3000 (Invitrogen) was used following the manufacturer's guidelines. Appropriate empty vectors were used as transfection control (TF-Ctrl). NIH3T3 cells were treated with 20 μM eupatilin (#SML1689; Sigma-Aldrich) or DMSO as a solvent control for 24 h.

Antibodies and plasmids

Cells were immunolabeled with primary antibodies targeting Arl13b (#17711-1-AP; Proteintech and #75-287; Antibodies Incorporated), Cep290 (#ab84870; Abcam), Cspp1 (#11931-1-AP; Proteintech), Flag (#F7425; Sigma-Aldrich), Myc (#sc-789; Santa Cruz Biotechnology), Nphp5 (#15747-1-AP; Proteintech), Sept2 (#11397-1-AP; Proteintech), Sept7 (#13818-1-AP; Proteintech), Sstr3 (#20696-1-AP; Proteintech; #PA3-207; Pierce Biotechnology and #11617; Santa Cruz Biotechnology), acetylated α-tubulin (#sc-23950; Santa Cruz Biotechnology; #T-6793; Sigma-Aldrich), and γ-tubulin (#sc-7396; Santa Cruz Biotechnology). The generation of the polyclonal antibody against Rpgrip1l was described formerly (Vierkotten *et al.*, 2007).

The following plasmids were used: pMyc-mNphp1 (kindly provided by Sophie Saunier), eGFP-hCEP290 (kindly provided by Hemant Khanna), and pFlag-mCep290 (#27381; Addgene). pMyc-mNphp1 encodes for the murine full-length Nphp1 protein fused to a Myc-tag (vector: CMV), GFP-hCEP290 encodes for the human full-length Cep290 protein fused to a GFP-tag (vector: CMV), and pFlag-mCep290 encodes for the murine full-length Cep290 protein fused to a Flag-tag (vector: CMV2).

CRISPR/Cas9-mediated gene inactivation

Inactivation of mouse *Rpgrip1l* in NIH3T3 cells was performed as previously described (Wiegering *et al.*, 2018a). We choose a target site which is located in exon3 of the gene (Supplemental Figure S2). After inactivation and single-cell cloning, eight clones, which on RFLP analysis appeared to have lost the diagnostic *Eag*I recognition sequence, were further analyzed. To establish the genotype, individual alleles were cloned and sequenced (Supplemental Figure S2).

Reagent or resource	Source	Identifier
Antibodies		
Rabbit polyclonal anti-Actin	Sigma-Aldrich	#A2066
Rabbit polyclonal anti-Arl13b	Proteintech	#17711-1-AP
Mouse monoclonal anti-Arl13b	Antibodies Incorporated	#75-287
Rabbit polyclonal anti-Cep290	Abcam	#ab84870
Rabbit polyclonal anti-Cspp1	Proteintech	#11931-1-AP
Rabbit polyclonal anti-Flag	Sigma-Aldrich	#F7425
Rabbit polyclonal anti-Gapdh	Abcam	#ab9485
Rabbit polyclonal anti-GFP	Thermo Fisher Scientific	#A-6455
Rabbit polyclonal anti-Nphp5/Iqcb1	Proteintech	#15747-1-AP
Rabbit polyclonal anti-c-Myc	Santa Cruz Biotechnology	#sc-789
Rabbit polyclonal anti-Sept2	Proteintech	#11397-1-AP
Rabbit polyclonal anti-Sept7	Proteintech	#13818-1-AP
Rabbit polyclonal anti-Sstr3	Proteintech	#20696-1-AP
Rabbit polyclonal anti-Sstr3	Pierce Biotechnology	#PA3-207
Goat polyclonal anti-Sstr3	Santa CruzBiotechnology	#sc-11617
Mouse monoclonal anti-acetylated α-Tubulin	Santa Cruz Biotechnology	#sc-23950
Mouse monoclonal anti-acetylated α-Tubulin	Sigma-Aldrich	#T-6739
Goat polyclonal anti-γ-Tubulin	Santa Cruz Biotechnology.	#sc-7396
Goat polyclonal anti-mouse IgG2b Alexa Fluor 488	Thermo Fisher Scientific	#A21141
Goat polyclonal anti-mouse IgG2a Alexa Fluor 488	Thermo Fisher Scientific	#A21131
Goat polyclonal anti-mouse IgG1 Alexa Fluor 488	Thermo Fisher Scientific	#A21121
Goat polyclonal anti-mouse IgG1 Alexa Fluor 568	Thermo Fisher Scientific	#A21124
Goat polyclonal anti-mouse IgG2b Alexa Fluor 594	Thermo Fisher Scientific	#21145
Goat polyclonal anti-mouse IgG2a Alexa Fluor 594	Thermo Fisher Scientific	#A21135
Donkey polyclonal anti-goat Dylight405	Jackson ImmunoResearch	#AB_2340426
Donkey polyclonal anti-mouse Alexa488	Jackson ImmunoResearch	#AB_2340846
Donkey polyclonal anit-rabbit Cy3	Jackson ImmunoResearch via Dianova	# 111-165-045
Chemicals, Peptides, and Recombinant Proteins		
DMSO	Sigma-Aldrich	#W387520
Eupatilin	Sigma-Aldrich	#SML1689
Experimental Models: Cell Lines		
HEK293	DSMZ	#ACC305
NIH3T3	DSMZ	#ACC59
Oligonucleotides		
Rpgrip1l-T3b-for: GAATGGCCACCAAGTTAATACGGCTAG	This study	N/A
Rpgrip1l-T3b-rev: CTTCAGGATCTGACAGAGAGCAAGCCTC	This study	N/A
T3 off-1 for: CTGTCAGGTTTCCCAGTGTGCAG	This study	N/A
T3 off-1 rev: CTCTCAGCTCCTTTTAGGTCTCCAG	This study	N/A

TABLE 1: Key resources. (Continues)

Reagent or resource	Source	Identifier
T3 off-2 for: ATCCAGCCAAACCCTGCCTGTTC	This study	N/A
T3 off-2 rev: GGTTTGTCTCTGTCCTGACATGTCAC	This study	N/A
T3 off-3 for: GTCTCCTTCAGACCCACTGAAGTG	This study	N/A
T3 off-3 rev: GTCCCAGGAAGCCAGGCTGTTG	This study	N/A
Recombinant DNA		
pMyc-mNphp1	Kindly provided by Sophie Saunier	N/A
pFlag-mCep290	Addgene	#27381
eGFP-hCEP290	Kindly provided by Hemant Khanna	N/A
Software and Algorithms		
ImageJ	National Institutes of Heath	https://imagej.nih.gov/ij
AxioVision Rel. 4.8 software package	Carl Zeiss AG	https://www.zeiss.de/mikroskopie
NIS-Elements	Nikon	https://www.microscope.healthcare.nikon.com
Adobe Photoshop CS2	Adobe	https://www.adobe.com
GraphPad Prism	GraphPad	https://www.graphpad.com

TABLE 1: Key resources. Continued

Sequences of the target site and primer pairs used to amplify the targeted region are as follows:

Rpgrip1l –T3: CTCGAGTTAACACCGGCCGCCGG

Rpgrip1l-T3b-for: GAATGGCCACCAAGTTAATACGGCTAG

Rpgrip1l-T3b-rev: CTTCAGGATCTGACAGAGAGCAAGCCTC.

Off-target analyses

Off-target analyses were performed by RFLP analyses as previously described (Wiegering *et al.*, 2018a). For the on-target Rpgrip1l-T3 there exist no off-targets carrying one, two, or three mismatches. From the remaining four-mismatch off-targets, we tested the top-three ranking sites (Hsu *et al.*, 2013) (crispr.mit.edu/) on the DNAs from the same eight-set clones analyzed for targeting of the on-target. In summary, we did not detect any mutations (unpublished data).

Sequences of the off-target sites and primer pairs used for amplification are as follows:

T3 offtarget-1: CACGAGTCAGCACCGGCCACTGG

T3 off-1 for: CTGTCAGGTTTCCCAGTGTGCAG

T3 off-1 rev: CTCTCAGCTCCTTTTAGGTCTCCAG

T3 offtarget-2: CTCTACTGAACAACGGCCGCAGG

T3 off-2 for: ATCCAGCCAAACCCTGCCTGTTC

T3 off-2 rev: GGTTTGTCTCTGTCCTGACATGTCAC

T3 offtarget-3: ATCCAGTTGACACCGGCCTCTGG

T3 off-3 for: GTCTCCTTCAGACCCACTGAAGTG

T3 off-3 rev: GTCCCAGGAAGCCAGGCTGTTG.

The following restriction enzymes were used: *Bsl*I (T3 off-target-1), *Eag*I (T3 off-target-2), and *Bsl*I (T3 off-target-1).

Image acquisition

Image acquisition and data analysis were carried out at room temperature using a Zeiss Imager.A2 microscope, 100×, NA 1.46 oil immersion objective lens (Carl Zeiss AG), a monochrome charge-coupled device camera (AxioCam MRm, Carl Zeiss AG), and the AxioVision Rel. 4.8 software package (Carl Zeiss AG), or a TI-Eclipse Nikon inverted microscope, 100×, 1.49 oil immersion objective lens coupled with a 95B Prime 22 mm Photometrics sCMOS camera. A Nikon fluorescent lamp and a quadriband dichroic block were used to detect blue, green, and red fluorescence. The acquisition software NIS was used. Three single-plane images per cilium were obtained in an 8-bit grayscale modus respectively covering the specific spectrum of the used fluorochrome. Appropriate anti-mouse, anti-rabbit and anti-goat Alexa405, Cy3, Alexa594, and Alexa488 antibodies were used as fluorochromes.

Immunofluorescence

For immunofluorescence on MEFs, NIH3T3 cells, and HEK293 cells, cells were plated on coverslips until confluency. MEFs and NIH3T3 cells were serum-starved for at least 24 h. Cells were fixed with 4% paraformaldehyde (for staining with the antibodies to Cep290, Rpgrip1l, Flag, Myc, Sept7, and Arl13b) or methanol (for staining with the antibodies to Cspp1, Nphp5, Sept2, and Sstr3). Fixed cells were rinsed three times with phosphate-buffered saline (PBS), followed by a permeabilization step with PBS/0.5% Triton X-100 for 10 min. The samples were rinsed three times with PBS. Samples were incubated for at least 10 min at room temperature in PBST (PBS/0.1% Triton X-100) containing 10% donkey serum or 10% normal goat serum. Diluted primary antibodies (in blocking solution) were incubated overnight at 4°C. After three washing steps with PBST, incubation with fluorescent secondary antibody (diluted in

blocking solution) was performed at room temperature for 1 h followed by several washing steps and subsequent embedding with Mowiol optionally containing DAPI.

Western blotting

Whole-cell lysates were obtained by lysis with radioimmunoprecipitation buffer (150 mM sodium chloride, 50 mM Tris-HCl, pH 7.4, 0.1% sodium deoxycholate, and 1 mM EDTA). Protein content was measured by the Bradford method, and samples were normalized. Total protein (20 mg) was separated by SDS–PAGE on polyacrylamide gels (#456-1093; Bio-Rad Laboratories) and transferred to a PVDF membrane (#162-0176; Bio-Rad). The membrane was probed with antibodies against Flag (#F7425; Sigma-Aldrich), GFP (#A-6455; Thermo Fisher Scientific), and Myc (#sc-789; Santa Cruz Biotechnology). Anti-Gapdh (#ab9485; Abcam) antibody was used as loading control. Proteins were detected with secondary antibodies conjugated to horseradish peroxidase (RPN4201 and RPN4301) and the SuperSignal West Pico PLUS detection kit (#34580; Thermo Fisher Scientific). Visualization of protein bands was realized by GBox (SYNGENE).

Quantification and presentation

Ciliary protein staining and protein bands intensity were quantified using ImageJ (National Institutes of Health). Intensity measurement of proteins based on immunofluorescence staining was performed as described before (Garcia-Gonzalo *et al.*, 2011; Garcia-Gonzalo *et al.*, 2015; Gerhardt *et al.*, 2015; Roberson *et al.*, 2015; Yee *et al.*, 2015; Struchtrup *et al.*, 2018; Wiegering *et al.*, 2018a). Triplets of 8-bit single-plane grayscale images were merged via ImageJ. The merged images were not further processed and the signal intensities were measured. The ciliary length has to be taken into account while quantifying the ciliary amount of Arl13b and Sstr3 in different genotypes. Therefore we used the area marked by acetylated α-tubulin as a reference and quantified the average pixel intensity of the Arl13 and Sstr3 staining. For all other ciliary protein intensities (Cep290, GFP, Flag, Cspp1, Myc, Nphp5, Rpgrip1l, Sept2, and Sept7), we selected the region labeled by γ-tubulin (for BB proteins) or the area in between the γ-tubulin staining and the proximal part of the acetylated α-tubulin staining and measured the total pixel intensity. To exclude unspecific staining from the measurements, we subtracted the mean value of the average pixel intensity (in the case of Arl13b and Sstr3) or of the total pixel intensity (all other ciliary proteins) of three neighboring regions free from specific staining.

Representative images were processed after quantification of ciliary protein staining was completed. The images were processed by means of background subtraction and contrast settings via Adobe Photoshop CS2.

Statistical analysis

Data are presented as mean ± SEM. Two-tailed *t* test with Welch´s correction was performed for all data in which two datasets were compared. Analysis of variance (ANOVA) and Tukey honest significance difference (HSD) tests were used for all data in which more than two datasets were compared. $*P < 0.05$ was considered to be statistically significant, $**P < 0.01$ was defined as statistically very significant, and $***P < 0.001$ was noted as statistically high significant. Sample sizes are indicated in the figure legends and the power of statistical tests was verified via post-hoc power calculations.

All statistical data analysis and graph illustrations were performed by using GraphPad Prism (GraphPad Software) and the Post-hoc Power Calculator (https://clincalc.com/Stats/).

DATA AND CODE AVAILABILITY

This study did not generate datasets.

ACKNOWLEDGMENTS

The authors thank Matias Zurbriggen and Leonie-Alexa Koch for their generous help to enable the continuation of the study. Moreover, we are grateful to Sophie Saunier for providing the Myc-mNphp1 construct. We thank the cell imaging facility of the IBPS (Institut de Biologie Paris-Seine FR3631, Sorbonne Université, CNRS, Paris, France) for their technical assistance. This work was funded by the Fondation ARC pour la Recherche sur le Cancer (Project ARC PJA 20171206591 to S.S.M.), the Fondation pour la Recherche Médicale (Equipe FRM EQU201903007943 to S.S.M.), and the German Research Foundation (DFG; Grant No. WI 5451/1-1 to A.W.).

REFERENCES

Andreu-Cervera A, Anselme I, Karam A, Laclef C, Catala M, Schneider-Maunoury S (2019). The ciliopathy gene ftm/rpgrip1l controls mouse forebrain patterning via region-specific modulation of hedgehog/gli signaling. J Neurosci 39, 2398–2415.

Assis L, Silva-Junior R, Dolce L, Alborghetti M, Honorato R, Nascimento A, Melo-Hanchuk T, Trindade D, Tonoli C, Santos C, *et al.* (2017). The molecular motor Myosin Va interacts with the cilia-centrosomal protein RPGRIP1L. Sci Rep 7, 43692.

Aubusson-Fleury A, Lemullois M, de Loubresse N, Laligné C, Cohen J, Rosnet O, Jerka-Dziadosz M, Beisson J, Koll F (2012). The conserved centrosomal protein FOR20 is required for assembly of the transition zone and basal body docking at the cell surface. J Cell Sci 125, 4395–4404.

Avasthi P, Marshall W (2012). Stages of ciliogenesis and regulation of ciliary length. Differentiation 83, 30–42.

Awata J, Takada S, Standley C, Lechtreck K, Bellvé K, Pazour G, Fogarty K, Witman G (2014). NPHP4 controls ciliary trafficking of membrane proteins and large soluble proteins at the transition zone. J Cell Sci 127, 4714–4727.

Bachmann-Gagescu R, Dona M, Hetterschijt L, Tonnaer E, Peters T, de Vrieze E, Mans D, van Beersum S, Phelps I, Arts H, *et al.* (2015). The ciliopathy protein CC2D2A associates with NINL and functions in RAB8-MICAL3-regulated vesicle trafficking. PLoS Genet 11, e1005575.

Barbelanne M, Hossain D, Chan D, Peränen J, Tsang W (2015a). Nephrocystin proteins NPHP5 and Cep290 regulate BBSome integrity, ciliary trafficking and cargo delivery. Hum Mol Genet 24, 2185–2200.

Barbelanne M, Hossain D, Chan D, Peränen J, Tsang W (2015b). Nephrocystin proteins NPHP5 and Cep290 regulate BBSome integrity, ciliary trafficking and cargo delivery. Hum Mol Genet 24, 2185–2200.

Barbelanne M, Song J, Ahmadzai M, Tsang W (2013). Pathogenic NPHP5 mutations impair protein interaction with Cep290, a prerequisite for ciliogenesis. Hum Mol Genet 22, 2482–2494.

Bärenz F, Inoue D, Yokoyama H, Tegha-Dunghu J, Freiss S, Draeger S, Mayilo D, Cado I, Merker S, Klinger M, *et al.* (2013). The centriolar satellite protein SSX2IP promotes centrosome maturation. J Cell Biol 202, 91–85.

Basiri M, Ha A, Chadha A, Clark N, Polyanovsky A, Cook B, Avidor-Reiss T (2014). A migrating ciliary gate compartmentalizes the site of axoneme assembly in Drosophila spermatids. Curr Biol 24, 2622–2631.

Benzing T, Schermer B (2011). Transition zone proteins and cilia dynamics. Nat Genet 43, 723–724.

Besse L, Neti M, Anselme I, Gerhardt C, Rüther U, Laclef C, Schneider-Maunoury S (2011). Primary cilia control telencephalic patterning and morphogenesis via Gli3 proteolytic processing. Development 138, 2079–2088.

Betleja E, Cole D (2010). Ciliary trafficking: CEP290 guards a gated community. Curr Biol 20, R928–R931.

Bonafé N, Sellers J (1998). Molecular characterization of myosin V from Drosophila melanogaster. J Muscle Res Cell Motil 19, 129–141.

Cevik S, Sanders A, Van Wijk E, Boldt K, Clarke L, van Reeuwijk J, Hori Y, Horn N, Hetterschijt L, Wdowicz A, *et al.* (2013). Active transport and diffusion barriers restrict Joubert Syndrome-associated ARL13B/ARL-13 to an Inv-like ciliary membrane subdomain. PLoS Genet 9, e1003977.

Chang B, Khanna H, Hawes N, Jimeno D, He S, Lillo C, Parapuram S, Cheng H, Scott A, Hurd R, *et al.* (2006). In-frame deletion in a novel

centrosomal/ciliary protein CEP290/NPHP6 perturbs its interaction with RPGR and results in early-onset retinal degeneration in the rd16 mouse. Hum Mol Genet 15, 1847–1857.
Chen J, Laclef C, Moncayo A, Snedecor E, Yang N, Li L, Takemaru K, Paus R, Schneider-Maunoury S, Clark R (2015). The ciliopathy gene Rpgrip1l is essential for hair follicle development. J Invest Dermatol 135, 701–709.
Chih B, Liu P, Chinn Y, Chalouni C, Komuves L, Hass P, Sandoval W, Peterson A (2011). A ciliopathy complex at the transition zone protects the cilia as a privileged membrane domain. Nat Cell Biol 14, 61–72.
Choi Y, Laclef C, Yang N, Andreu-Cervera A, Lewis J, Mao X, Li L, Snedecor E, Takemaru K, Qin C, *et al.* (2019). RPGRIP1L is required for stabilizing epidermal keratinocyte adhesion through regulating desmoglein endocytosis. PLoS Genet 15, e1007914.
Coene K, Mans D, Boldt K, Gloeckner C, van Reeuwijk J, Bolat E, Roosing S, Letteboer S, Peters T, Cremers F, *et al.* (2011). The ciliopathy-associated protein homologs RPGRIP1 and RPGRIP1L are linked to cilium integrity through interaction with Nek4 serine/threonine kinase. Hum Mol Genet 20, 3592–3605.
Copeland J (2020). Actin-based regulation of ciliogenesis - The long and the short of it. Semin Cell Dev Biol 102, 132–138.
Craige B, Tsao C, Diener D, Hou Y, Lechtreck K, Rosenbaum J, Witman G (2010). CEP290 tethers flagellar transition zone microtubules to the membrane and regulates flagellar protein content. J Cell Biol 190, 927–940.
Czarnecki PG, Shah JV (2012). The ciliary transition zone: from morphology and molecules to medicine. Trends Cell Biol 22, 201–210.
Damerla R, Cui C, Gabriel G, Liu X, Craige B, Gibbs B, Francis R, Li Y, Chatterjee B, San Agustin J, *et al.* (2015). Novel Jbts17 mutant mouse model of Joubert syndrome with cilia transition zone defects and cerebellar and other ciliopathy related anomalies. Hum Mol Genet 24, 3994–4005.
Dammermann A, Merdes A (2002). Assembly of centrosomal proteins and microtubule organization depends on PCM-1. J Cell Biol 159, 255–266.
Delous M, Baala L, Salomon R, Laclef C, Vierkotten J, Tory K, Golzio C, Lacoste T, Besse L, Ozilou C, *et al.* (2007). The ciliary gene RPGRIP1L is mutated in cerebello-oculo-renal syndrome (Joubert syndrome type B) and Meckel syndrome. Nat Genet 39, 875–881.
Dyson J, Conduit S, Feeney S, Hakim S, DiTommaso T, Fulcher A, Sriratana A, Ramm G, Horan K, Gurung R, *et al.* (2017). INPP5E regulates phosphoinositide-dependent cilia transition zone function. J Cell Biol 216, 247–263.
Garcia-Gonzalo F, Corbit K, Sirerol-Piquer M, Ramaswami G, Otto E, Noriega T, Seol A, Robinson J, Bennett C, Josifova D, *et al.* (2011). A transition zone complex regulates mammalian ciliogenesis and ciliary membrane composition. Nat Genet 43, 776–784.
Garcia-Gonzalo F, Phua S, Roberson E, Garcia Gr, Abedin M, Schurmans S, Inoue T, Reiter J (2015). Phosphoinositides regulate ciliary protein trafficking to modulate hedgehog signaling. Dev Cell 34, 400–409.
Garcia-Gonzalo F, Reiter J (2012). Scoring a backstage pass: Mechanisms of ciliogenesis and ciliary access. J Cell Biol 197, 697–709.
Garcia-Gonzalo F, Reiter J (2017). Open sesame: how transition fibers and the transition zone control ciliary composition. Cold Spring Harb Perspect Biol 9, pii: a028134.
Gerhardt C, Lier J, Burmühl S, Struchtrup A, Deutschmann K, Vetter M, Leu T, Reeg S, Grune T, Rüther U (2015). The transition zone protein Rpgrip1l regulates proteasomal activity at the primary cilium. J Cell Biol 210, 115–133.
Gerhardt C, Lier J, Kuschel S, Rüther U (2013). The ciliary protein Ftm is required for ventricular wall and septal development. PLoS One 8, e57545.
Gupta G, Coyaud E, Gonçalves J, Mojarad B, Liu Y, Wu Q, Gheiratmand L, Comartin D, Tkach J, Cheung S, *et al.* (2015). A dynamic protein interaction landscape of the human centrosome-cilium interface. Cell 163, 1484–1499.
Händel M, Schulz S, Stanarius A, Schreff M, Erdtmann-Vourliotis M, Schmidt H, Wolf G, Höllt V (1999). Selective targeting of somatostatin receptor 3 to neuronal cilia. Neuroscience 89, 909–926.
Helou J, Otto E, Attanasio M, Allen S, Parisi M, Glass I, Utsch B, Hashmi S, Fazzi E, Omran H, *et al.* (2007). Mutation analysis of NPHP6/CEP290 in patients with Joubert syndrome and Senior-Løken syndrome. J Med Genet 44, 657–663.
Hildebrandt F, Benzing T, Katsanis N (2011). Ciliopathies. N Engl J Med 364, 1533–1543.
Hori A, Ikebe C, Tada M, Toda T (2014). Msd1/SSX2IP-dependent microtubule anchorage ensures spindle orientation and primary cilia formation. EMBO Rep 15, 175–184.
Hori A, Peddie C, Collinson L, Toda T (2015). Centriolar satellite- and hMsd1/SSX2IP-dependent microtubule anchoring is critical for centriole assembly. Mol Biol Cell 26, 2005–2019.
Hsu P, Scott D, Weinstein J, Ran F, Konermann S, Agarwala V, Li Y, Fine E, Wu X, Shalem O, *et al.* (2013). DNA targeting specificity of RNA-guided Cas9 nucleases. Nat Biotechnol 31, 827–832.
Hu Q, Milenkovic L, Jin H, Scott M, Nachury M, Spiliotis E, Nelson W (2010). A septin diffusion barrier at the base of the primary cilium maintains ciliary membrane protein distribution. Science 329, 436–439.
Huang L, Szymanska K, Jensen V, Janecke A, Innes A, Davis E, Frosk P, Li C, Willer J, Chodirker B, *et al.* (2011). TMEM237 is mutated in individuals with a Joubert syndrome related disorder and expands the role of the TMEM family at the ciliary transition zone. Am J Hum Genet 89, 713–730.
Hynes A, Giles R, Srivastava S, Eley L, Whitehead J, Danilenko M, Raman S, Slaats G, Colville J, Ajzenberg H, *et al.* (2014). Murine Joubert syndrome reveals Hedgehog signaling defects as a potential therapeutic target for nephronophthisis. Proc Natl Acad Sci USA 111, 9893–9898.
Ishikawa H, Marshall W (2011). Ciliogenesis: building the cell's antenna. Nat Rev Mol Cell Biol 12, 222–234.
Jack B, Mueller D, Fee A, Tetlow A, Avasthi P. (2019). Partially redundant actin genes in chlamydomonas control transition zone organization and flagellum-directed traffic. Cell Rep 27, 2459–2467.e2453.
Jensen V, Lambacher N, Li C, Mohan S, Williams C, Inglis P, Yoder B, Blacque O, Leroux M (2018). Role for intraflagellar transport in building a functional transition zone. EMBO Rep 19, pii: e45862.
Jensen V, Leroux M (2017). Gates for soluble and membrane proteins, two trafficking systems (IFT and LIFT), establish a dynamic ciliary signaling compartment. Curr Opin Cell Biol 47, 83–91.
Jensen V, Li C, Bowie R, Clarke L, Mohan S, Blacque O, Leroux M (2015). Formation of the transition zone by Mks5/Rpgrip1L establishes a ciliary zone of exclusion (CIZE) that compartmentalises ciliary signalling proteins and controls PIP2 ciliary abundance. EMBO J 34, 2537–2556.
Jiang S, Chiou Y, Wang E, Chien Y, Ho H, Tsai F, Lin C, Tsai S, Li H (2009). Essential role of nephrocystin in photoreceptor intraflagellar transport in mouse. Hum Mol Genet 18, 1566–1577.
Jiang S, Chiou Y, Wang E, Lin H, Lee S, Lu H, Wang C, Tang M, Li H (2008). Targeted disruption of Nphp1 causes male infertility due to defects in the later steps of sperm morphogenesis in mice. Hum Mol Genet 17, 3368–3379.
Keeling J, Tsiokas L, Maskey D. (2016). Cellular mechanisms of ciliary length control. Cells. 5, 6.
Kilander M, Wang C, Chang C, Nestor J, Herold K, Tsai J, Nestor M, Lin Y (2018). A rare human CEP290 variant disrupts the molecular integrity of the primary cilium and impairs Sonic Hedgehog machinery. Sci Rep 8, 17335.
Kim Y, Kim S, Jung Y, Jung E, Kwon H, Kim J (2018). Eupatilin Rescues Ciliary Transition Zone Defects to Ameliorate Ciliopathy-Related Phenotypes. J Clin Invest 128, 3642–3648.
Kim J, Krishnaswami S, Gleeson J (2008). CEP290 interacts with the centriolar satellite component PCM-1 and is required for Rab8 localization to the primary cilium. Hum Mol Genet 17, 3796–3805.
Klinger M, Wang W, Kuhns S, Bärenz F, Dräger-Meurer S, Pereira G, Gruss O (2014). The novel centriolar satellite protein SSX2IP targets Cep290 to the ciliary transition zone. Mol Biol Cell 25, 495–507.
Kobayashi T, Kim S, Lin Y, Inoue T, Dynlacht B (2014). The CP110-interacting proteins Talpid3 and Cep290 play overlapping and distinct roles in cilia assembly. J Cell Biol 204, 215–229.
Kohli P, Höhne M, Jüngst C, Bertsch S, Ebert L, Schauss A, Benzing T, Rinschen M, Schermer B (2017). The ciliary membrane-associated proteome reveals actin-binding proteins as key components of cilia. EMBO Rep 18, 1521–1535.
Kubo A, Sasaki H, Yuba-Kubo A, Tsukita S, Shiina N (1999). Centriolar satellites: molecular characterization, ATP-dependent movement toward centrioles and possible involvement in ciliogenesis. J Cell Biol 147, 969–980.
Kubo A, Tsukita S (2003). Non-membranous granular organelle consisting of PCM-1: subcellular distribution and cell-cycle-dependent assembly/disassembly. J Cell Sci 116, 919–928.
Kumar D, Reiter J (2020). How the centriole builds its cilium: of mothers, daughters, and the acquisition of appendages. Curr Opin Struct Biol 66, 41–48.
Laclef C, Anselme I, Besse L, Catala M, Palmyre A, Baas D, Paschaki M, Pedraza M, Métin C, Durand B, Schneider-Maunoury S (2015). The role of primary cilia in corpus callosum formation is mediated by production of the Gli3 repressor. Hum Mol Genet 24, 4997–5014.

Lambacher N, Bruel A, van Dam T, Szymańska K, Slaats G, Kuhns S, McManus G, Kennedy J, Gaff K, Wu K, *et al.* (2016). TMEM107 recruits ciliopathy proteins to subdomains of the ciliary transition zone and causes Joubert syndrome. Nat Cell Biol 18, 122–131.

Lancaster M, Gopal D, Kim J, Saleem S, Silhavy J, Louie C, Thacker B, Williams Y, Zaki M, Gleeson J (2011). Defective Wnt-dependent cerebellar midline fusion in a mouse model of Joubert syndrome. Nat Med 17, 726–731.

Lapart J, Gottardo M, Cortier E, Duteyrat J, Augière C, Mangé A, Jerber J, Solassol J, Gopalakrishnan J, Thomas J, Durand B (2019). Dzip1 and Fam92 form a ciliary transition zone complex with cell type specific roles in Drosophila. Elife 8, e49307.

Lewis W, Bales K, Revell D, Croyle M, Engle S, Song C, Malarkey E, Uytingco C, Shan D, Antonellis P, *et al.* (2019). Mks6 mutations reveal tissue- and cell type-specific roles for the cilia transition zone. FASEB J 33, 1440–1455.

Li C, Jensen V, Park K, Kennedy J, Garcia-Gonzalo F, Romani M, De Mori R, Bruel A, Gaillard D, Doray B, *et al.* (2016). MKS5 and CEP290 dependent assembly pathway of the ciliary transition zone. PLoS Biol 14, e1002416.

Li Y, Klena N, Gabriel G, Liu X, Kim A, Lemke K, Chen Y, Chatterjee B, Devine W, Damerla R, *et al.* (2015). Global genetic analysis in mice unveils central role for cilia in congenital heart disease. Nature 521, 520–524.

Lin H, Guo S, Dutcher S (2018). RPGRIP1L helps to establish the ciliary gate for entry of proteins. J Cell Sci 131, pii: jcs220905.

Louie C, Caridi G, Lopes V, Brancati F, Kispert A, Lancaster M, Schlossman A, Otto E, Leitges M, Gröne H, *et al.* (2010). AHI1 is required for photoreceptor outer segment development and is a modifier for retinal degeneration in nephronophthisis. Nat Genet 42, 175–180.

Lu H, Galeano M, Ott E, Kaeslin G, Kausalya P, Kramer C, Ortiz-Brüchle N, Hilger N, Metzis V, Hiersche M, *et al.* (2017). Mutations in DZIP1L, which encodes a ciliary-transition-zone protein, cause autosomal recessive polycystic kidney disease. Nat Genet 49, 1025–1034.

Madhivanan K, Aguilar R (2014). Ciliopathies: the trafficking connection. Traffic 15, 1031–1056.

McEwen D, Koenekoop R, Khanna H, Jenkins P, Lopez I, Swaroop A, Martens J (2007). Hypomorphic CEP290/NPHP6 mutations result in anosmia caused by the selective loss of G proteins in cilia of olfactory sensory neurons. Proc Natl Acad Sci USA 104, 15917–15922.

McIntyre J, Williams C, Martens J (2013). Smelling the roses and seeing the light: gene therapy for ciliopathies. Trends Biotechnol 31, 355–363.

Mitchison H, Valente E (2017). Motile and non-motile cilia in human pathology: from function to phenotypes. J Pathol 241, 294–309.

Mochizuki T, Saijoh Y, Tsuchiya K, Shirayoshi Y, Takai S, Taya C, Yonekawa H, Yamada K, Nihei H, Nakatsuji N, *et al.* (1998). Cloning of inv, a gene that controls left/right asymmetry and kidney development. Nature 395, 177–181.

Molinari E, Ramsbottom S, Srivastava S, Booth P, Alkanderi S, McLafferty S, Devlin L, White K, Gunay-Aygun M, Miles C, Sayer J (2019). Targeted exon skipping rescues ciliary protein composition defects in Joubert syndrome patient fibroblasts. Sci Rep 9, 10828.

Morgan D, Turnpenny L, Goodship J, Dai W, Majumder K, Matthews L, Gardner A, Schuster G, Vien L, Harrison W, *et al.* (1998). Inversin, a novel gene in the vertebrate left-right axis pathway, is partially deleted in the inv mouse. Nat Genet 20, 149–156.

Mukherjee I, Roy S, Chakrabarti S (2019). Identification of important effector proteins in the FOXJ1 transcriptional network associated with ciliogenesis and ciliary function. Front Genet 10, 23.

Nachury M, Loktev A, Zhang Q, Westlake C, Peränen J, Merdes A, Slusarski D, Scheller R, Bazan J, Sheffield V, Jackson P. (2007). A core complex of BBS proteins cooperates with the GTPase Rab8 to promote ciliary membrane biogenesis. Cell 129, 1201–1213.

Odabasi E, Gul S, Kavakli I, Firat-Karalar E (2019). Centriolar satellites are required for efficient ciliogenesis and ciliary content regulation. EMBO Rep. 20, e47723.

Omran H (2010). NPHP proteins: gatekeepers of the ciliary compartment. J Cell Biol 190, 715–717.

Otto E, Loeys B, Khanna H, Hellemans J, Sudbrak R, Fan S, Muerb U, O'Toole J, Helou J, Attanasio M, *et al.* (2005). Nephrocystin-5, a ciliary IQ domain protein, is mutated in Senior-Loken syndrome and interacts with RPGR and calmodulin. Nat Genet 37, 282–288.

Patnaik S, Zhang X, Biswas L, Akhtar S, Zhou X, Kusuluri D, Reilly J, May-Simera H, Chalmers S, McCarron J, Shu X (2018). RPGR protein complex regulates proteasome activity and mediates store-operated calcium entry. Oncotarget 9, 23183–23197.

Patzke S, Redick S, Warsame A, Murga-Zamalloa C, Khanna H, Doxsey S, Stokke T (2010). CSPP is a ciliary protein interacting with Nephrocystin 8 and required for cilia formation. Mol Biol Cell 21, 2555–2567.

Pocha S, Shevchenko A, Knust E (2011). Crumbs regulates rhodopsin transport by interacting with and stabilizing myosin V. J Cell Biol 195, 827–838.

Pratt M, Titlow J, Davis I, Barker A, Dawe H, Raff J, Roque H (2016). Drosophila sensory cilia lacking MKS proteins exhibit striking defects in development but only subtle defects in adults. J Cell Sci 129, 3732–3743.

Rachel R, Yamamoto E, Dewanjee M, May-Simera H, Sergeev Y, Hackett A, Pohida K, Munasinghe J, Gotoh N, Wickstead B, *et al.* (2015). CEP290 alleles in mice disrupt tissue-specific cilia biogenesis and recapitulate features of syndromic ciliopathies. Hum Mol Genet 24, 3775–3791.

Reiter J, Blacque O, Leroux M (2012). The base of the cilium: roles for transition fibres and the transition zone in ciliary formation, maintenance and compartmentalization. EMBO Rep 13, 608–618.

Reiter J, Leroux M (2017). Genes and molecular pathways underpinning ciliopathies. Nat Rev Mol Cell Biol 18, 533–547.

Reiter J, Skarnes W (2006). Tectonic, a novel regulator of the Hedgehog pathway required for both activation and inhibition. Genes Dev 20, 22–27.

Roberson E, Dowdle W, Ozanturk A, Garcia-Gonzalo F, Li C, Halbritter J, Elkhartoufi N, Porath J, Cope H, Ashley-Koch A, *et al.* (2015). TMEM231, mutated in orofaciodigital and Meckel syndromes, organizes the ciliary transition zone. J Cell Biol 209, 129–142.

Ronquillo C, Hanke-Gogokhia C, Revelo M, Frederick J, Jiang L, Baehr W (2016). Ciliopathy-associated IQCB1/NPHP5 protein is required for mouse photoreceptor outer segment formation. FASEB J 30, 3400–3412.

Sang L, Miller J, Corbit K, Giles R, Brauer M, Otto E, Baye L, Wen X, Scales S, Kwong M, *et al.* (2011). Mapping the NPHP-JBTS-MKS protein network reveals ciliopathy disease genes and pathways. Cell 145, 513–528.

Scheidel N, Blacque O (2018). Intraflagellar transport complex A genes differentially regulate cilium formation and transition zone gating. Curr Biol 28, 3279–3287.e3272.

Schou K, Mogensen J, Morthorst S, Nielsen B, Aleliunaite A, Serra-Marques A, Fürstenberg N, Saunier S, Bizet A, Veland I, *et al.* (2017). KIF13B establishes a CAV1-enriched microdomain at the ciliary transition zone to promote Sonic hedgehog signalling. Nat Commun 8, 14177.

Shaheen R, Shamseldin H, Loucks C, Seidahmed M, Ansari S, Ibrahim Khalil M, Al-Yacoub N, Davis E, Mola N, Szymanska K, *et al.* (2014). Mutations in CSPP1, encoding a core centrosomal protein, cause a range of ciliopathy phenotypes in humans. Am J Hum Genet 94, 73–79.

Shi X, Garcia Gr, Van De Weghe J, McGorty R, Pazour G, Doherty D, Huang B, Reiter J (2017). Super-resolution microscopy reveals that disruption of ciliary transition-zone architecture causes Joubert syndrome. Nat Cell Biol 19, 1178–1188.

Shimada H, Lu Q, Insinna-Kettenhofen C, Nagashima K, English M, Semler E, Mahgerefteh J, Cideciyan A, Li T, Brooks B, *et al.* (2017). In Vitro modeling using ciliopathy-patient-derived cells reveals distinct cilia dysfunctions caused by CEP290 mutations. Cell Rep 20, 384–396.

Slaats G, Isabella C, Kroes H, Dempsey J, Gremmels H, Monroe G, Phelps I, Duran K, Adkins J, Kumar S, *et al.* (2016). MKS1 regulates ciliary INPP5E levels in Joubert syndrome. J Med Genet 53, 62–72.

Stone E, Cideciyan A, Aleman T, Scheetz T, umaroka A, Ehlinger M, Schwartz S, Fishman G, Traboulsi E, Lam B, *et al.* (2011). Variations in NPHP5 in patients with nonsyndromic leber congenital amaurosis and Senior-Loken Syndrome. Arch Ophthalmol 129, 81–87.

Stowe T, Wilkinson C, Iqbal A, Stearnsa T (2012). The centriolar satellite proteins Cep72 and Cep290 interact and are required for recruitment of BBS proteins to the cilium. Mol Biol Cell 23, 3322–3335.

Struchtrup A, Wiegering A, Stork B, Rüther U, Gerhardt C (2018). The ciliary protein RPGRIP1L governs autophagy independently of its proteasome-regulating function at the ciliary base in mouse embryonic fibroblasts. Autophagy 14, 567–583.

Szymanska K, Johnson C (2012). The transition zone: an essential functional compartment of cilia. Cilia 1, 10.

Takao D, Wang L, Boss A, Verhey K (2017). Protein interaction analysis provides a map of the spatial and temporal organization of the ciliary gating zone. Curr Biol 27, 2296–2306.e2293.

Tsang W, Bossard C, Khanna H, Peränen J, Swaroop S, Malhotra V, Dynlacht B (2008). CP110 suppresses primary cilia formation through its interaction with CEP290, a protein deficient in human ciliary disease. Dev Cell 15, 187–197.

Tuz K, Bachmann-Gagescu R, O'Day D, Hua K, Isabella C, Phelps I, Stolarski A, O'Roak B, Dempsey J, Lourenco C, *et al*. (2014). Mutations in CSPP1 cause primary cilia abnormalities and Joubert syndrome with or without Jeune asphyxiating thoracic dystrophy. Am J Hum Genet 94, 62–72.
Vieillard J, Paschaki M, Duteyrat J, Augière C, Cortier E, Lapart J, Thomas J, Durand B (2016). Transition zone assembly and its contribution to axoneme formation in Drosophila male germ cells. J Cell Biol 214, 875–889.
Vierkotten J, Dildrop R, Peters T, Wang B, Rüther U (2007). Ftm is a novel basal body protein of cilia involved in Shh signalling. Development 134, 2569–2577.
Wang L, Dynlacht B (2018). The regulation of cilium assembly and disassembly in development and disease. Development 145, dev151407.
Wang W, Tay H, Soni R, Perumal G, Goll M, Macaluso F, Asara J, Amack J, Tsou M (2013). CEP162 is an axoneme-recognition protein promoting ciliary transition zone assembly at the cilia base. Nat Cell Biol 15, 591–601.
War S, Kumar U (2012). Coexpression of human somatostatin receptor-2 (SSTR2) and SSTR3 modulates antiproliferative signaling and apoptosis. J Mol Signal 7, 5.
Warburton-Pitt S, Jauregui A, Li C, Wang J, Leroux M, Barr M (2012). Ciliogenesis in Caenorhabditis elegans requires genetic interactions between ciliary middle segment localized NPHP-2 (inversin) and transition zone-associated proteins. J Cell Sci 125, 2592–2603.
Wei Q, Zhang Y, Schouteden C, Zhang Y, Zhang Q, Dong J, Wonesch V, Ling K, Dammermann A, Hu J (2016). The hydrolethalus syndrome protein HYLS-1 regulates formation of the ciliary gate. Nat Commun 7, 12437.
Weng R, Yang T, Huang C, Chang C, Wang W, Liao J (2018). Super-Resolution Imaging Reveals TCTN2 Depletion-Induced IFT88 Lumen Leakage and Ciliary Weakening. Biophys J 115, 263–275.
Wiegering A, Dildrop R, Kalfhues L, Spychala A, Kuschel S, Lier J, Zobel T, Dahmen S, Leu T, Struchtrup A, *et al*. (2018a). Cell type-specific regulation of ciliary transition zone assembly in vertebrates. EMBO J 37, pii: e97791.
Wiegering A, Rüther U, Gerhardt C (2018b). The ciliary protein Rpgrip1l in development and disease. Dev Biol 442, 60–68.
Williams C, Li C, Kida K, Inglis P, Mohan S, Semenec L, Bialas N, Stupay R, Chen N, Blacque O, *et al*. (2011). MKS and NPHP modules cooperate to establish basal body/transition zone membrane associations and ciliary gate function during ciliogenesis. J Cell Biol 192, 1023–1041.
Won J, Marín de Evsikova C, Smith R, Hicks W, Edwards M, Longo-Guess C, Li T, Naggert J, Nishina P (2011). NPHP4 is necessary for normal photoreceptor ribbon synapse maintenance and outer segment formation, and for sperm development. Hum Mol Genet 20, 482–496.
Wu C, Chen H, Tang T (2018). Myosin-Va is required for preciliary vesicle transportation to the mother centriole during ciliogenesis. Nat Cell Biol 20, 175–185.
Ye F, Nager A, Nachury M (2018). BBSome trains remove activated GPCRs from cilia by enabling passage through the transition zone. J Cell Biol 217, 1847–1868.
Yee L, Garcia-Gonzalo F, Bowie R, Li C, Kennedy J, Ashrafi K, Blacque O, Leroux M, Reiter J (2015). Conserved genetic interactions between ciliopathy complexes cooperatively support ciliogenesis and ciliary signaling. PLoS Genet 11, e1005627.
Yoshimura S, Egerer J, Fuchs E, Haas A, Barr F (2007). Functional dissection of Rab GTPases involved in primary cilium formation. J Cell Biol 178, 363–369.
Zaghloul N, Katsanis N (2010). Functional modules, mutational load and human genetic disease. Trends Genet 26, 168–176.
Zuo X, Guo W, Lipschutz J (2009). The exocyst protein Sec10 is necessary for primary ciliogenesis and cystogenesis in vitro. Mol Biol Cell 20, 2522–2529.